Supplement of Earth Syst. Sci. Data, 17, 3167–3187, 2025
https://doi.org/10.5194/essd-17-3167-2025-supplement
© Author(s) 2025. CC BY 4.0 License.

Supplement of

A dataset of ground-based vertical profile observations of aerosol, NO_2, and HCHO from the hyperspectral vertical remote sensing network in China (2019–2023)

Peiyuan Jiao et al.

Correspondence to: Chengzhi Xing (xingcz@aiofm.ac.cn) and Cheng Liu (chliu81@ustc.edu.cn)

The copyright of individual parts of the supplement might differ from the article licence.

Section S1. Data Filtering Criteria and Principles

DOF (Degrees of Freedom): In the retrieval process, the averaging kernel matrix reflects the sensitivity of the observation data to the state vector transformation. The sum of the diagonal elements of this matrix represents the Degrees of Freedom (DOF), which quantifies the amount of independent information that can be effectively extracted from the observational data. A higher DOF indicates that more independent information has been extracted, whereas a lower DOF suggests that the observation data is not sensitive to changes in the state vector. Consequently, we exclude data with a DOF value lower than 1.0, as this typically indicates that the retrieval process has not effectively utilized the observational data, leading to potentially unreliable results or higher uncertainty.

χ^2 (Chi-Square): As shown in Equation (1), the χ^2 value is used to assess the model fit, i.e., the difference between the model predictions and the actual observed values. A smaller χ^2 value indicates that the model closely matches the observed values, while a larger χ^2 value suggests a significant discrepancy, which may arise from inaccurate prior information, systematic errors, or other unaccounted factors. In order to ensure the quality and reliability of the analysis, we exclude data with χ^2 values greater than 200. This threshold helps to minimize the influence of outliers and ensures that the results are based on high-quality data.

$$\chi^2 = \left(\boldsymbol{y} - F(\boldsymbol{x}, \boldsymbol{b})\right)^T \boldsymbol{S}_{\varepsilon}^{-1}\left(\boldsymbol{y} - F(\boldsymbol{x}, \boldsymbol{b})\right) + (\boldsymbol{x} - \boldsymbol{x_a})^T \boldsymbol{S_a}^{-1}(\boldsymbol{x} - \boldsymbol{x_a}) \,, \tag{1}$$

SZA (Solar Zenith Angle): In this study, we focus on the absorption in the troposphere near the Earth's surface. When the solar zenith angle (SZA) exceeds 75°, the predominant scattering transpire within the lower stratosphere and upper troposphere (Song et al., 2023).

In this case, DOAS measurements exhibit heightened sensitivity towards stratospheric absorption, while demonstrating reduced sensitivity to absorption in the proximity of the surface. Therefore, measurements with SZA > 75° are excluded from the analysis.

CI (Color Index): The color index (CI) is defined as the ratio of the spectral intensities at 330 nm and 390 nm, and is used to identify potential cloud interference (Wagner et al., 2016). A polynomial function of time is fitted to the data from clear days without significant cloud cover to establish the diurnal CI variation pattern. Based on this fitted model, a CI threshold is determined for each time point. If the CI value at a given time is below 10% of the threshold, it is assumed that the data are affected by cloud interference, and such data are excluded from further analysis (Ryan et al., 2018).

Relative Retrieval Error: The relative retrieval error measures the precision of the retrieval results. If the relative error exceeds 50%, the result is considered to have too high an uncertainty and is therefore excluded as unreliable data (Tan et al., 2018).

Due to the peculiarity of the instrument's data collection and storage process, data with SZA and CI values that do not meet the criteria are excluded prior to processing. After filtering based on DOF, χ^2, and relative retrieval error, approximately 10% of the data is discarded.

Section S2. Time Series Analysis

Figures S1–S3 display the time series of aerosol extinction coefficient, NO_2 concentration, and HCHO concentration in the lower, middle, and upper layers between 2019 and 2023. The results indicate that the overall trends of the three pollutants in the upper atmosphere are generally consistent with those in the middle and lower layers. However, at certain sites and during specific periods, the trends in the lower layers may deviate from those in the middle and upper layers. Notably, interannual variations in pollutant concentrations are less pronounced in the upper atmosphere, whereas seasonal variations and diurnal patterns are more evident. Furthermore, the concentration fluctuations in the lower layers of the three pollutants are significantly greater than those in the middle and upper layers, and their concentration levels differ notably from those in the upper layers, with the most noticeable differences observed in the NO_2 time series. To quantify these differences, we calculated the ratios of average concentrations between altitude layers. For aerosols, the ratio of aerosol extinction coefficient in the upper layer to that in the lower layer is 33.09%, while the ratio in the middle layer to the lower layer is 64.36%. For NO_2, these values are 15.29% and 32.98%, respectively, while for HCHO, the corresponding ratios are 56.36% and 80.88%. Among the three pollutants, HCHO exhibits the smallest vertical gradient, indicating that its concentration differences and fluctuations across the lower, middle, and upper layers are relatively minimal. This suggests a more uniform vertical distribution of HCHO compared to aerosols and NO_2.

Table S1. The site type and the major emission sources around each site.

No.	Region	Site(code)	Site Type	Major emission sources
1	North China	Chinese Academy of Meteorological Sciences (CAMS)	Urban	Traffic emissions, residential heating, industrial activities
2		The Institute of Atmospheric Physics (IAP)	Urban	Traffic emissions, residential heating, industrial activities
3		Nancheng (NC)	Suburban	Agricultural activities, light industrial emissions
4		University of Chinese Academy of Sciences (UCAS)	Suburban	Traffic emissions, residential heating
5		Wangdu (WD)	Rural	Agricultural activities, biomass burning
6		Xianghe (XH)	Rural	Agricultural activities, biomass burning
7		Shijiazhuang (SJZ)	Urban	Heavy industrial emissions, traffic emissions, residential heating
8		Shanxi University (SXU)	Urban	Industrial emissions, traffic emissions
9		Inner Mongolia Normal University (IMNU)	High-altitude	Dust emissions, agricultural activities
10	East China	Dongying (DY)	Coastal	Oil refineries, petrochemical industries, traffic emissions
11		Qingdao (QD)	Coastal	Ship emissions, industrial activities, traffic emissions
12		Taishan (TS)	High-altitude	Background site, minimal local emissions
13		Tai'an(TA)	Urban	Traffic emissions, industrial activities
14		Shanghai_Xuhui (SH_XH)	Urban	Heavy traffic emissions, industrial activities, residential heating
15		Shanghai_Dianshan Lake (SH_DL)	Lakeside	Traffic emissions, industrial activities, ship emissions
16		Nanjing University of Information Science and Technology (NUIST)	Coastal	Traffic emissions, industrial activities, ship emissions
17		Ningbo (NB)	Coastal	Ship emissions, industrial activities, traffic emissions
18		Huaniao Island (HNI)	Coastal	Ship emissions, minimal local emissions
19		Lin'an(LA)	Rural	Agricultural activities, biomass burning
20		Huaibei Normal University (HNU)	Urban	Industrial emissions, traffic emissions
21		Anhui University (AHU)	Urban	Traffic emissions, industrial activities
22		Changfeng(CF)	Suburban	Traffic emissions, agricultural activities
23	South China	Xiamen_Institute of Urban Environment (IUE)	Urban	Traffic emissions, industrial activities, ship emissions
24		Guangzhou Institute of Geochemistry (GIG)	Urban	Traffic emissions, industrial activities, ship emissions
25		Southern University of Science and Technology (SUST)	Urban	Traffic emissions, industrial activities
26	Southwest China	Shangri-La Station (SLS)	High-altitude	Background site, minimal local emissions
27		Chongqing (CQ)	Urban	Heavy industrial emissions, traffic emissions
28	Northwest China	Lanzhou University (LZU)	Urban	Industrial emissions, traffic emissions, dust storms
29		Xi'an (XA)	Urban	Traffic emissions, industrial activities
30	Northeast China	Juehua Island (JHI)	Coastal	Ship emissions, minimal local emissions
31		Liaoning University (LNU)	Urban	Industrial emissions, traffic emissions
32	Central China	Luoyang (LY)	Urban	Heavy industrial emissions, traffic emissions

Table S2. The site observation period. The months listed in the observation period indicate that the site has data for a certain month. The specific monthly data integrity is shown in Figure 3.

No.	Region	Site(code)	Observation period	No.	Region	Site(code)	Observation period
1	North China	Chinese Academy of Meteorological Sciences (CAMS)	2019.01-2021.02 2021.04-2021.07 2021.10-2023.10 2021.04-2021.07	17	East China	Ningbo (NB)	2019.11-2020.01 2020.05-2020.06 2020.08-2021.03 2021.05-2021.06 2021.09-2021.09 2021.12-2021.12
2		The Institute of Atmospheric Physics (IAP)	2019.09-2021.03 2021.05-2021.05	18		Huaniao Island (HNI)	2019.04-2019.08 2019.11-2020.07 2020.11-2022.04
3		Nancheng (NC)	2019.01-2020.01 2020.05-2021.03 2021.07-2021.10 2021.12-2022.05	19		Lin’an(LA)	2020.12-2020.12 2021.02-2022.07
4		University of Chinese Academy of Sciences (UCAS)	2019.01-2020.02 2020.06-2021.07 2021.11-2022.07 2022.09-2023.05	20		Huaibei Normal University (HNU)	2020.06-2022.05
5		Wangdu (WD)	2019.03-2023.03 2023.06-2023.12	21		Anhui University (AHU)	2020.12-2023.09
6		Xianghe (XH)	2019.01-2019.01 2019.03-2019.10 2020.01-2021.05 2021.08-2022.01 2022.05-2022.05	22		Changfeng(CF)	2022.05-2022.12 2023.03-2023.12
7		Shijiazhuang (SJZ)	2019.10-2021.03 2021.05-2022.05	23	South China	Xiamen_Institute of Urban Environment (IUE)	2020.01-2020.03 2020.06-2020.09 2021.04-2021.05
8		Shanxi University (SXU)	2020.10-2020.11 2021.04-2022.03 2022.07-2023.07 2023.09-2023.12	24		Guangzhou Institute of Geochemistry (GIG)	2019.09-2021.10 2022.03-2023.11
9		Inner Mongolia Normal University (IMNU)	2020.07-2021.10 2022.01-2022.08 2023.10-2023.10	25		Southern University of Science and Technology (SUST)	2019.01-2021.11 2022.01-2022.12
10	East China	Dongying (DY)	2019.09-2019.09 2019.11-2020.05 2020.10-2021.07	26	Southwest China	Shangri-La Station (SLS)	2019.11-2022.08
11		Qingdao (QD)	2019.12-2020.12	27		Chongqing (CQ)	2019.01-2020.03 2020.05-2023.01 2023.03-2023.04
12		Taishan (TS)	2020.01-2020.02 2020.04-2022.07 2023.03-2023.03	28	Northwest China	Lanzhou University (LZU)	2019.01-2021.11
13		Tai’an(TA)	2021.06-2021.06 2021.08-2021.08 2021.12-2022.01	29		Xi’an (XA)	2020.01-2020.06 2020.08-2020.08
14		Shanghai_Xuhui (SH_XH)	2019.09-2020.01 2020.03-2020.12	30	Northeast China	Juehua Island (JHI)	2020.09-2021.06
15		Shanghai_Dianshan Lake (SH_DL)	2019.01-2019.06	31		Liaoning University (LNU)	2019.07-2019.07 2019.09-2019.12
16		Nanjing University of Information Science and Technology (NUIST)	2019.01-2019.07 2019.09-2019.11 2022.04-2023.12	32	Central China	Luoyang (LY)	2020.02-2022.02

Table S3. Differences in the data before and after filtering based on DOF, χ^2, and relative retrieval error, using the CAMS and HNI stations as examples. The numbers in the table represent the monthly data integrity at each site, indicating the ratio of days with and without data in a month.

	CAMS	CAMS (filtered)	HNI	HNI (filtered)
2019-01	1.00	1.00	0.00	0.00
2019-02	1.00	1.00	0.00	0.00
2019-03	0.94	0.94	0.00	0.00
2019-04	0.67	0.67	0.07	0.07
2019-05	0.87	0.87	0.06	0.06
2019-06	0.97	0.97	0.97	0.97
2019-07	1.00	1.00	1.00	0.97
2019-08	0.42	0.42	0.48	0.48
2019-09	0.43	0.43	0.00	0.00
2019-10	0.94	0.94	0.00	0.00
2019-11	1.00	1.00	0.97	0.97
2019-12	0.68	0.68	0.94	0.94
2020-01	0.94	0.94	1.00	1.00
2020-02	0.97	0.97	1.00	1.00
2020-03	1.00	1.00	1.00	1.00
2020-04	1.00	1.00	0.93	0.93
2020-05	1.00	1.00	0.94	0.94
2020-06	1.00	1.00	1.00	0.97
2020-07	1.00	1.00	0.39	0.39
2020-08	1.00	1.00	0.00	0.00
2020-09	0.97	0.97	0.00	0.00
2020-10	0.97	0.97	0.00	0.00
2020-11	0.83	0.83	0.93	0.90
2020-12	0.97	0.97	1.00	1.00
2021-01	0.97	0.97	0.94	0.94
2021-02	0.93	0.93	0.79	0.79
2021-03	0.00	0.00	0.52	0.52
2021-04	0.27	0.27	0.27	0.27
2021-05	0.97	0.97	0.77	0.77
2021-06	0.97	0.97	0.80	0.80
2021-07	0.48	0.48	0.84	0.84
2021-08	0.00	0.00	0.81	0.81
2021-09	0.00	0.00	0.43	0.43
2021-10	0.65	0.65	0.16	0.16
2021-11	0.77	0.77	0.67	0.67
2021-12	1.00	1.00	1.00	1.00
2022-01	0.97	0.97	0.81	0.81
2022-02	1.00	1.00	0.96	0.96
2022-03	1.00	1.00	1.00	1.00

2022-04	0.20	0.20	0.67	0.67
2022-05	0.55	0.55	0.00	0.00
2022-06	1.00	1.00	0.00	0.00
2022-07	1.00	1.00	0.00	0.00
2022-08	1.00	1.00	0.00	0.00
2022-09	1.00	1.00	0.00	0.00
2022-10	1.00	1.00	0.00	0.00
2022-11	0.97	0.97	0.00	0.00
2022-12	0.45	0.45	0.00	0.00
2023-01	1.00	0.97	0.00	0.00
2023-02	0.57	0.57	0.00	0.00
2023-03	1.00	1.00	0.00	0.00
2023-04	0.87	0.87	0.00	0.00
2023-05	0.90	0.90	0.00	0.00
2023-06	0.97	0.97	0.00	0.00
2023-07	0.97	0.97	0.00	0.00
2023-08	0.90	0.90	0.00	0.00
2023-09	0.77	0.77	0.00	0.00
2023-10	0.29	0.29	0.00	0.00

Table S4. The Sites location and their corresponding nearest China National Environmental Monitoring Center (CNEMC) stations.

	MAX-DOAS stations			The nearest CNEMCs		Distance (km)
No.	Station(code)	Longitude(°E)	Latitude(°N)	Longitude(°E)	Latitude(°N)	
1	CAMS	116.32	39.94	116.34	39.93	2.52
2	IAP	116.37	39.97	116.40	39.98	1.92
3	NC	116.12	39.78	116.15	39.82	4.95
4	UCAS	116.67	40.40	116.63	40.33	9.80
5	WD	115.15	38.17	114.85	38.03	30.38
6	XH	116.97	39.76	117.30	39.72	28.58
7	SJZ	114.60	37.90	114.64	37.90	2.94
8	SXU	112.58	37.63	112.56	37.74	12.09
9	IMNU	111.68	40.80	111.66	40.80	2.52
10	DY	118.98	37.76	118.57	37.57	42.01
11	QD	120.67	36.34	120.61	36.44	11.54
12	TS	117.10	36.25	117.09	36.20	6.11
13	TA	117.06	36.20	117.09	36.20	2.49
14	SH_XH	121.43	31.17	121.41	31.17	2.11
15	SH_DL	120.97	31.09	120.98	31.09	0.02
16	NUIST	118.71	32.20	118.81	32.11	14.16
17	NB	121.89	29.75	121.84	29.91	18.60
18	HNI	122.67	30.86	121.80	31.05	86.33
19	LA	119.75	30.30	119.72	32.24	7.43
20	HNU	116.80	33.98	116.80	33.98	1.03
21	AHU	117.18	31.77	117.20	31.78	1.80

22	CF	117.18	32.21	117.27	31.94	30.59
23	IUE	118.05	24.61	118.10	24.57	6.03
24	GIG	113.35	23.15	113.32	23.13	4.23
25	SUST	113.99	22.59	114.03	22.62	4.22
26	SLS	99.72	28.00	99.71	27.83	19.61
27	CQ	106.50	29.60	106.46	29.57	5.57
28	LZU	103.85	36.04	103.83	36.05	2.10
29	XA	109.09	34.52	109.00	34.26	1.04
30	JHI	120.77	40.47	120.83	40.71	26.25
31	LNU	123.04	41.81	123.40	41.79	1.64
32	LY	112.45	34.67	112.44	34.67	1.58

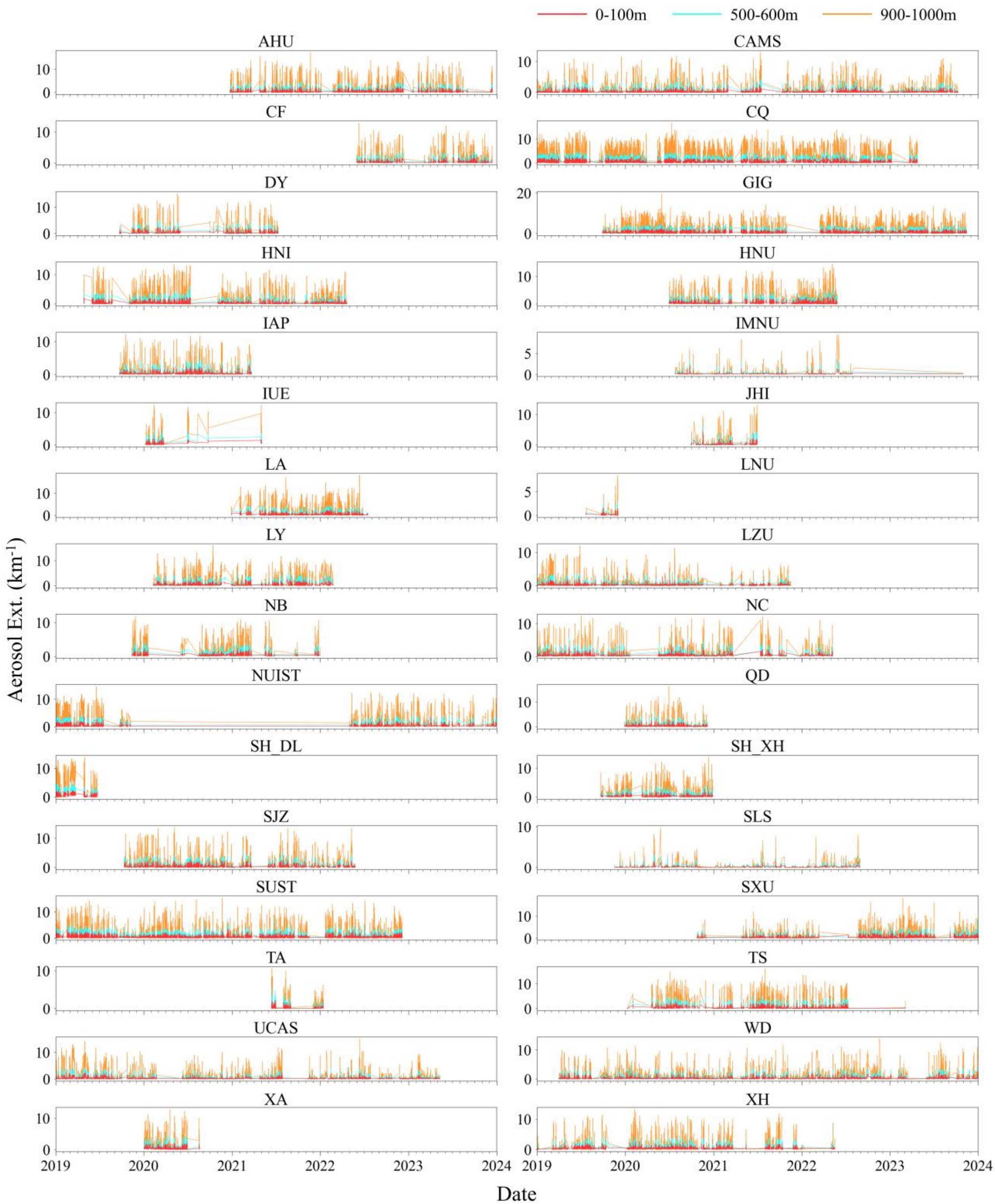

55 **Figure S1. Time series of aerosol extinction during 2019-2023.**

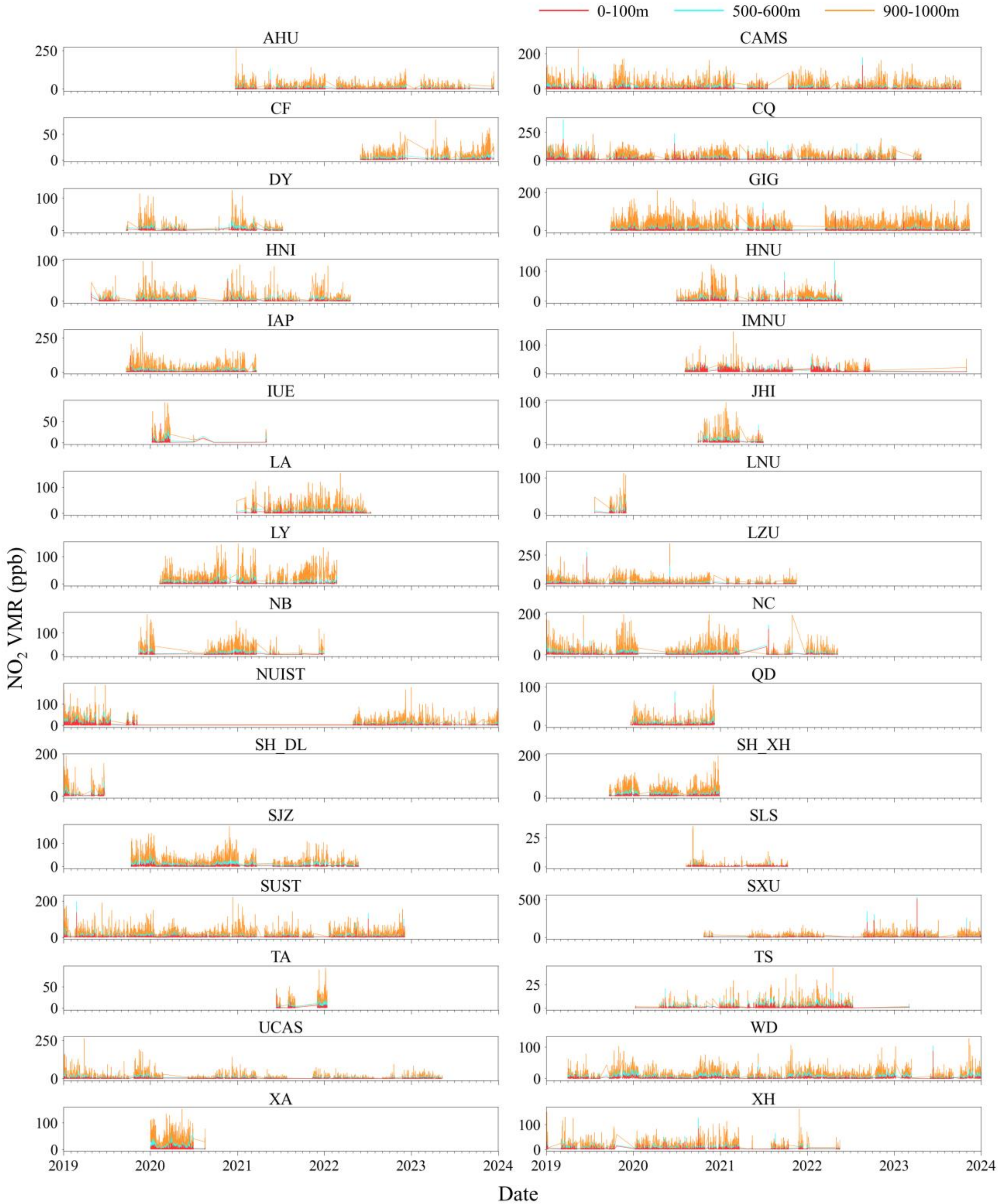

Figure S2. Time series of NO_2 concentration during 2019-2023.

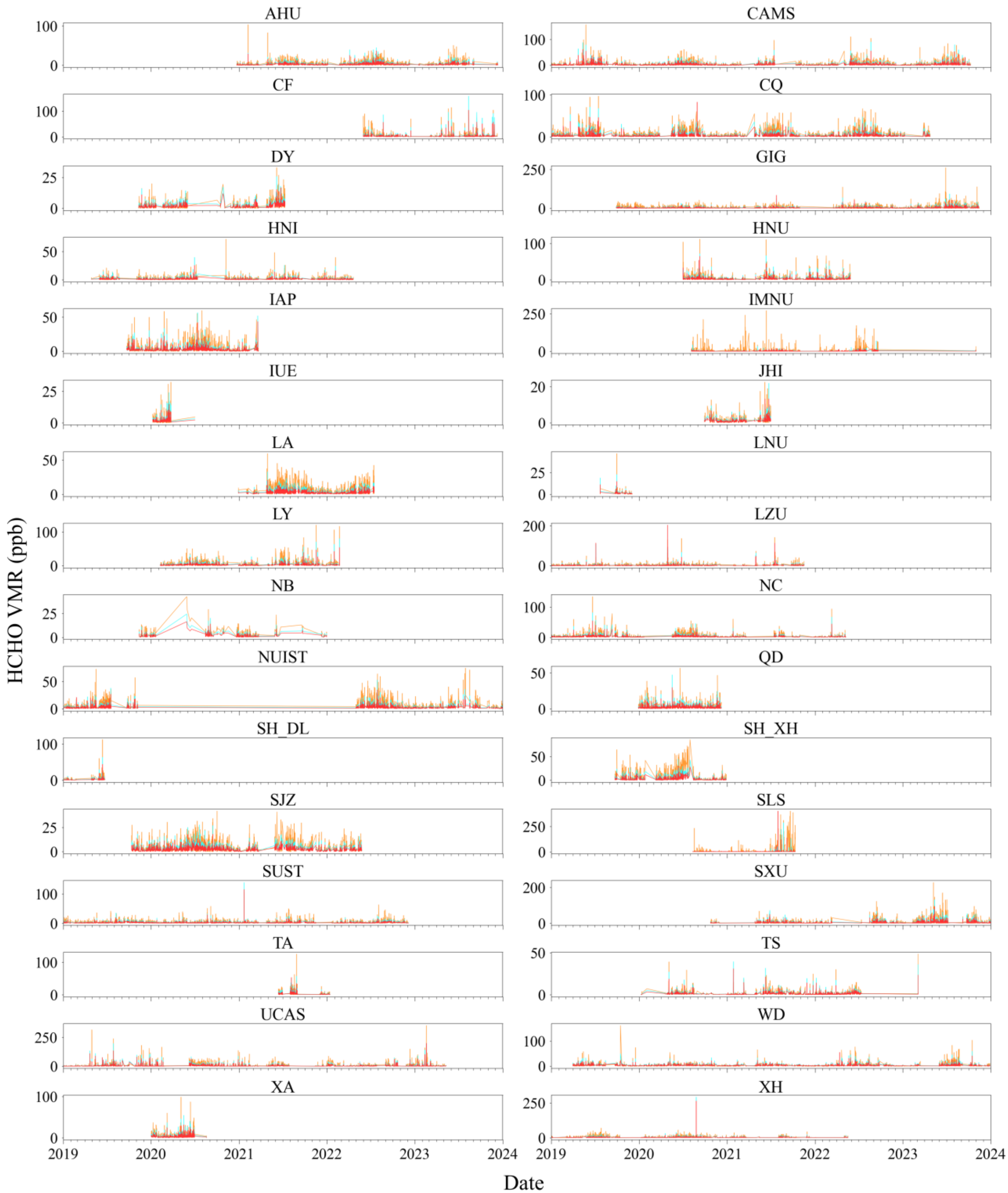

Figure S3. Time series of HCHO concentration during 2019-2023.

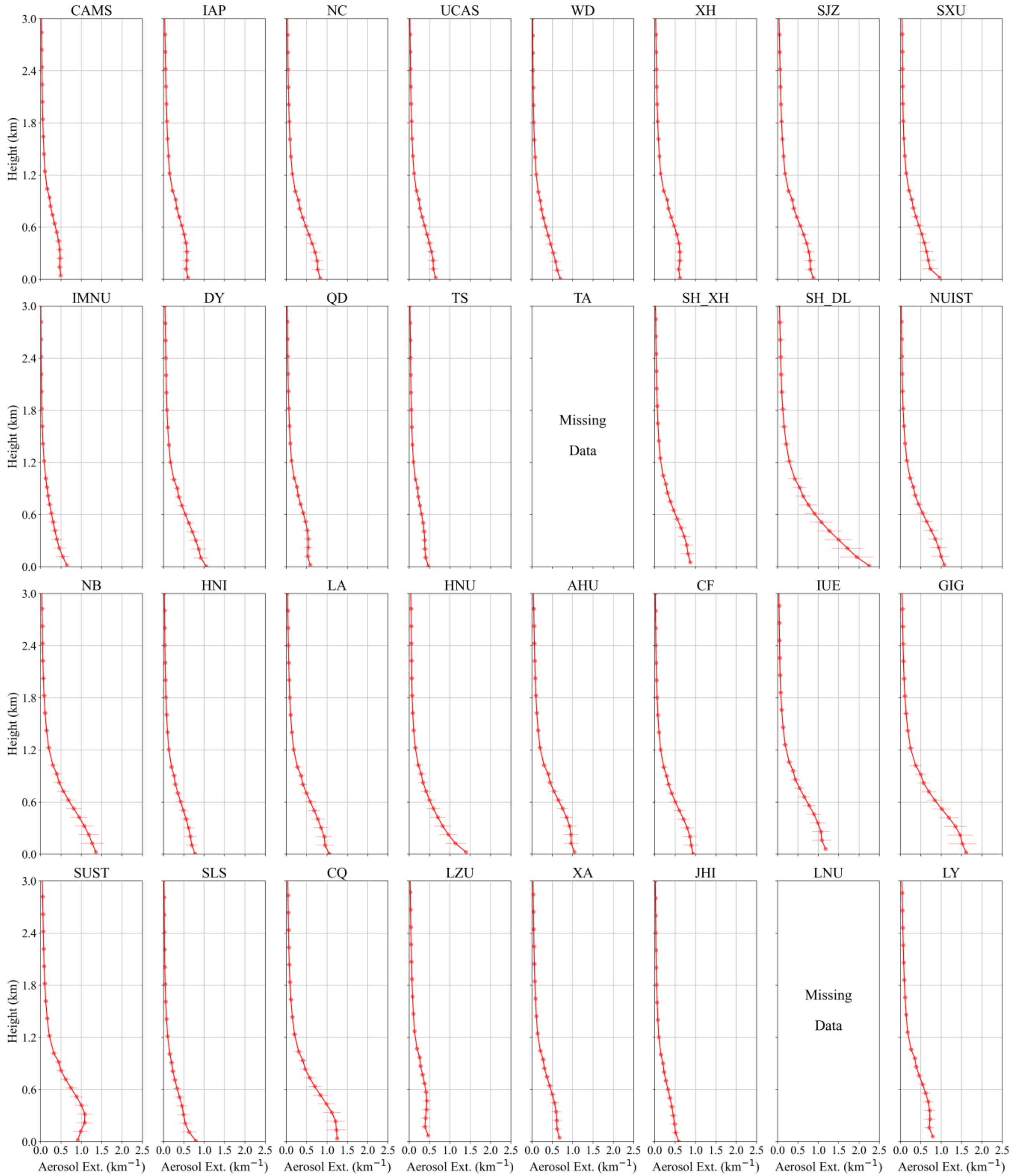

Figure S4. Spring averaged aerosol extinction vertical profiles during 2019-2023.

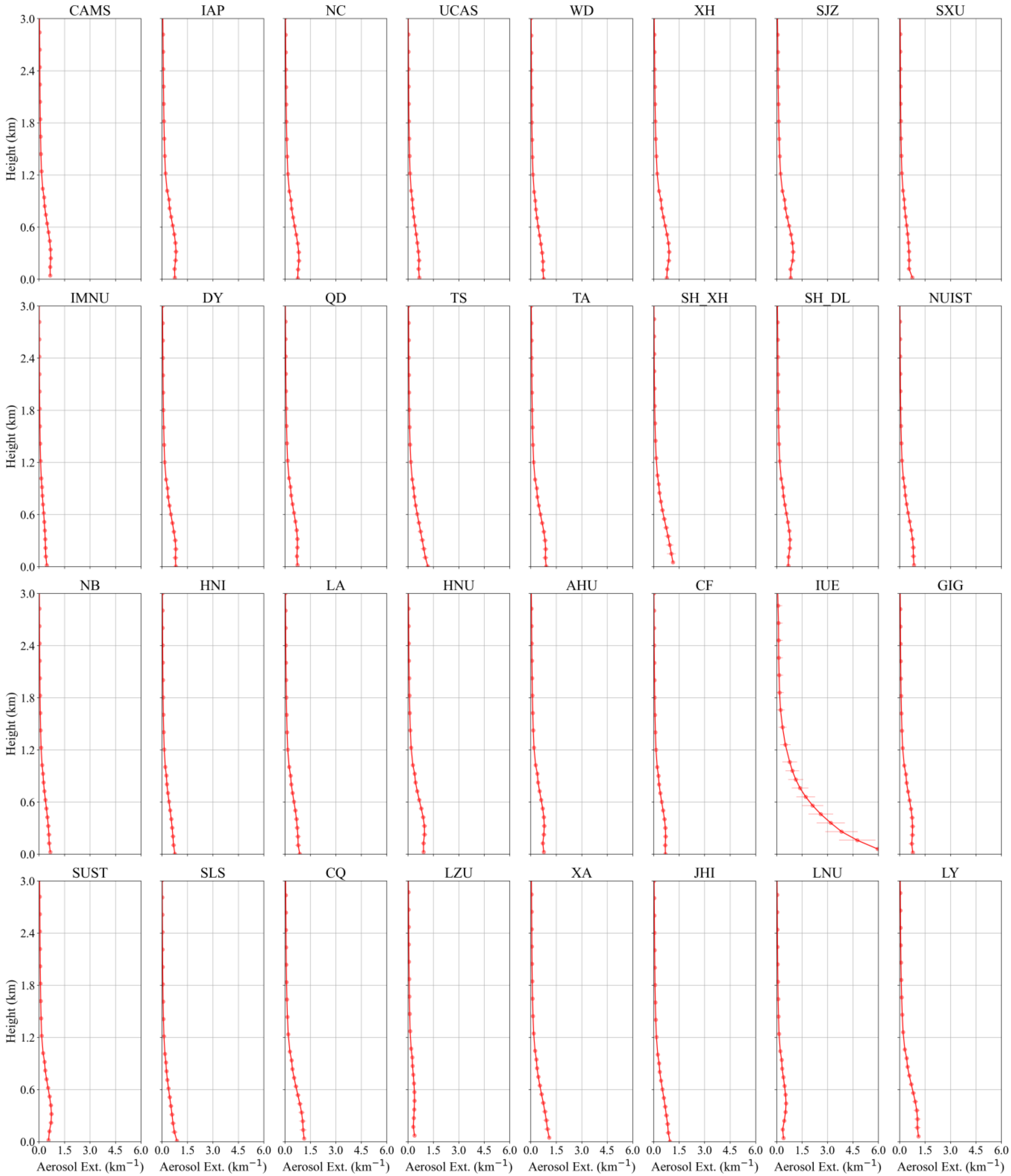

Figure S5. Summer averaged aerosol extinction vertical profiles during 2019-2023.

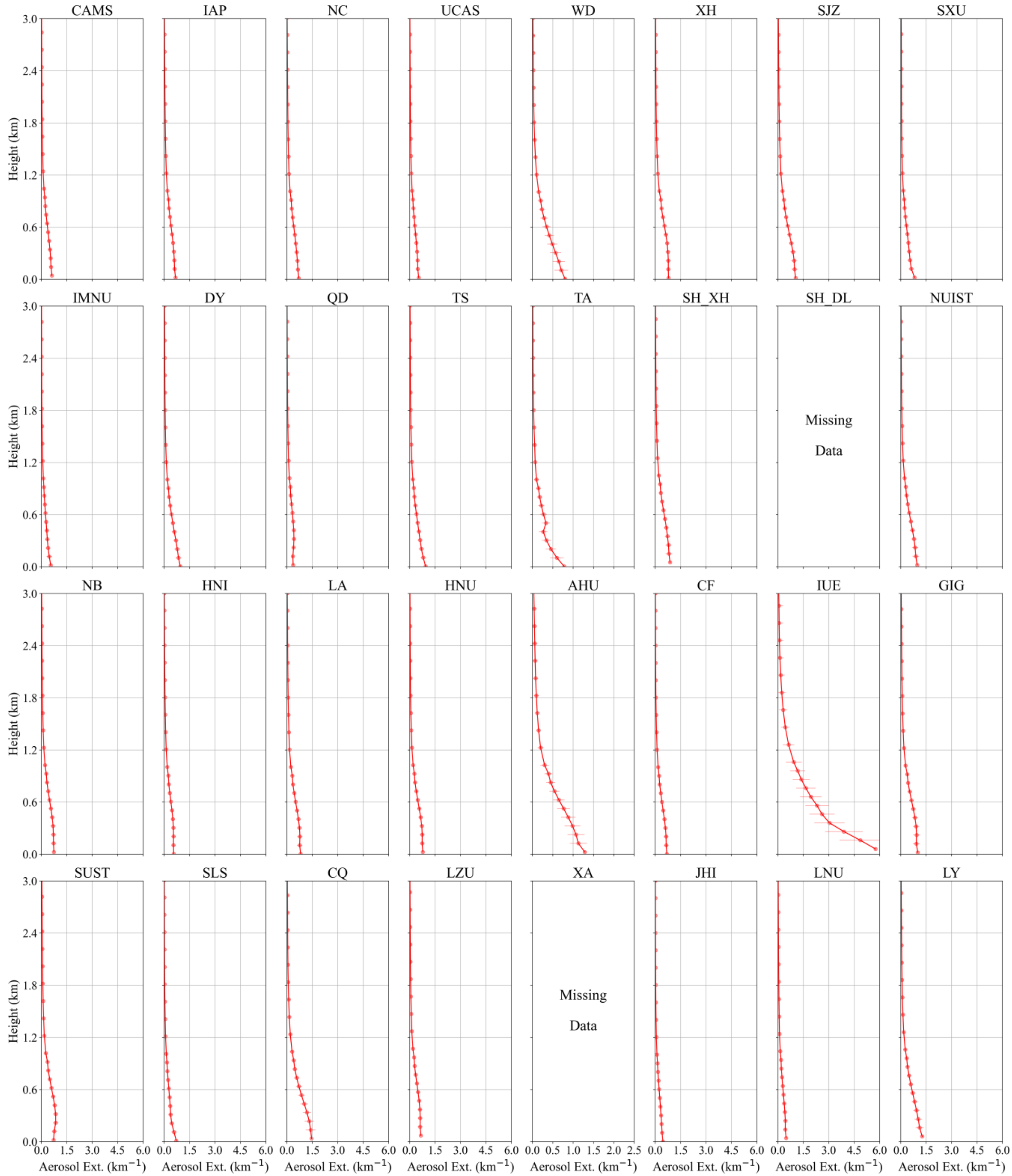

65 **Figure S6. Autumn averaged aerosol extinction vertical profiles during 2019-2023.**

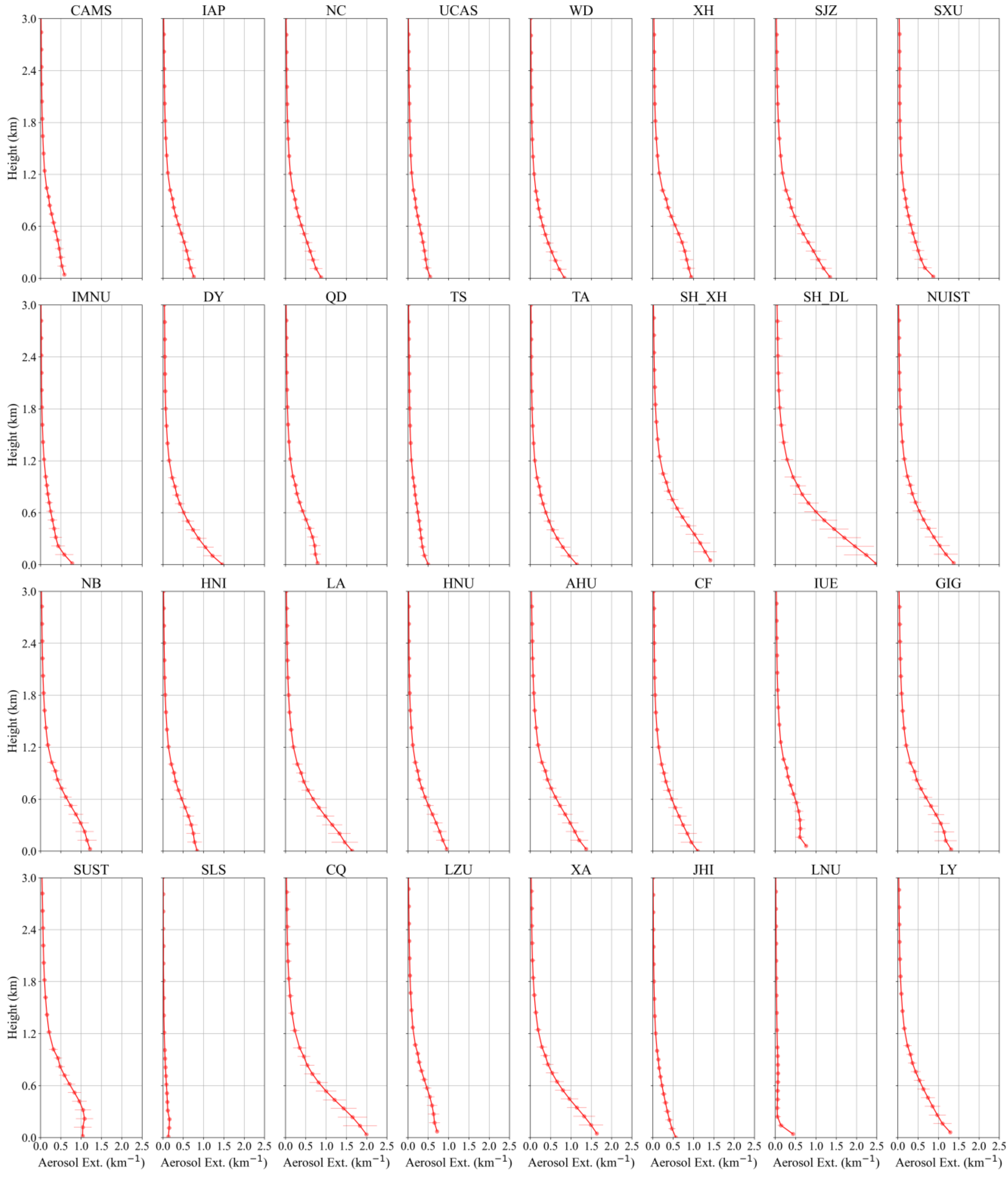

Figure S7. Winter averaged aerosol extinction vertical profiles during 2019-2023.

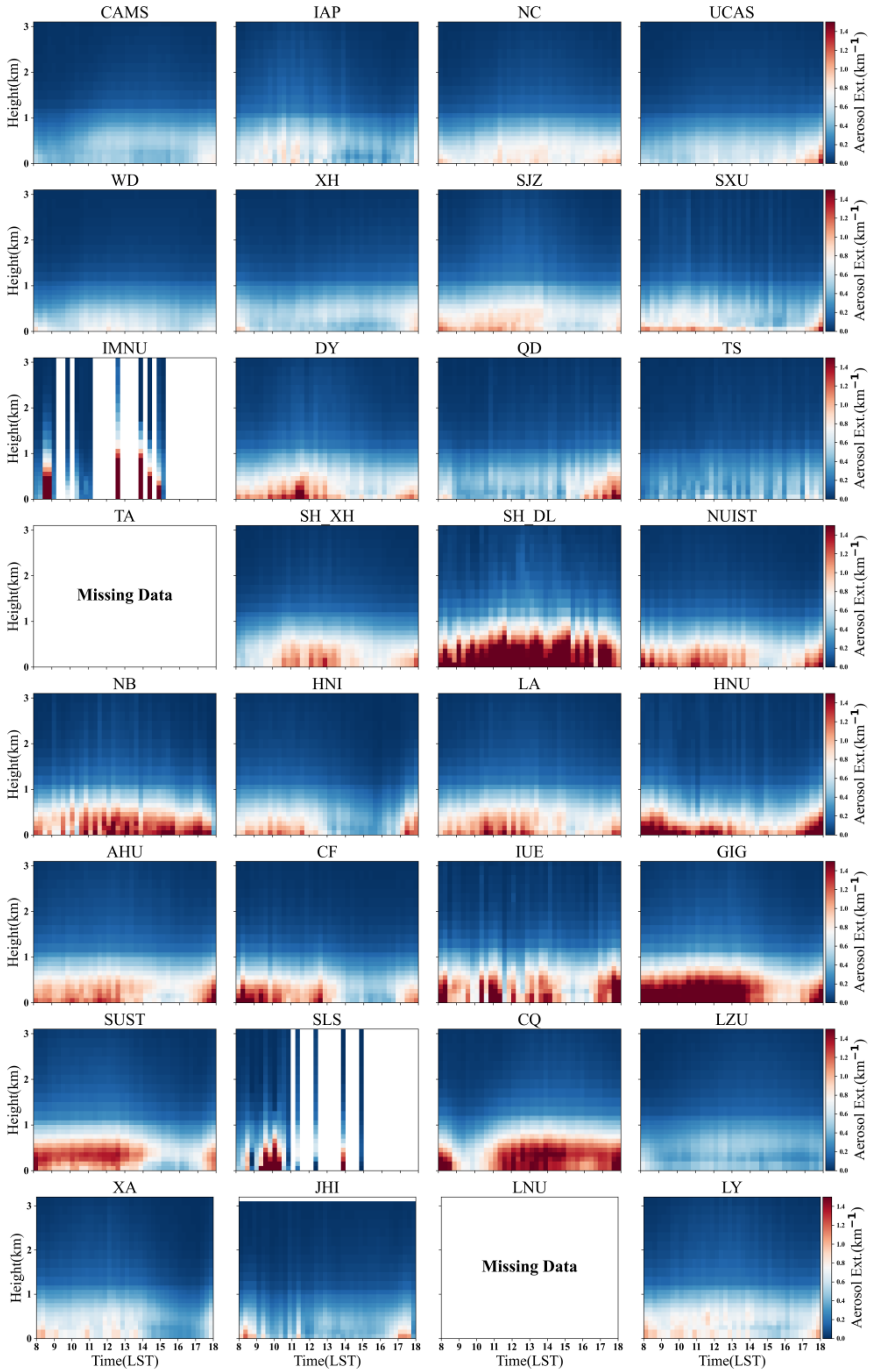

Figure S8. Diurnal variation of the spring averaged aerosol extinction vertical profiles during 2019-2023.

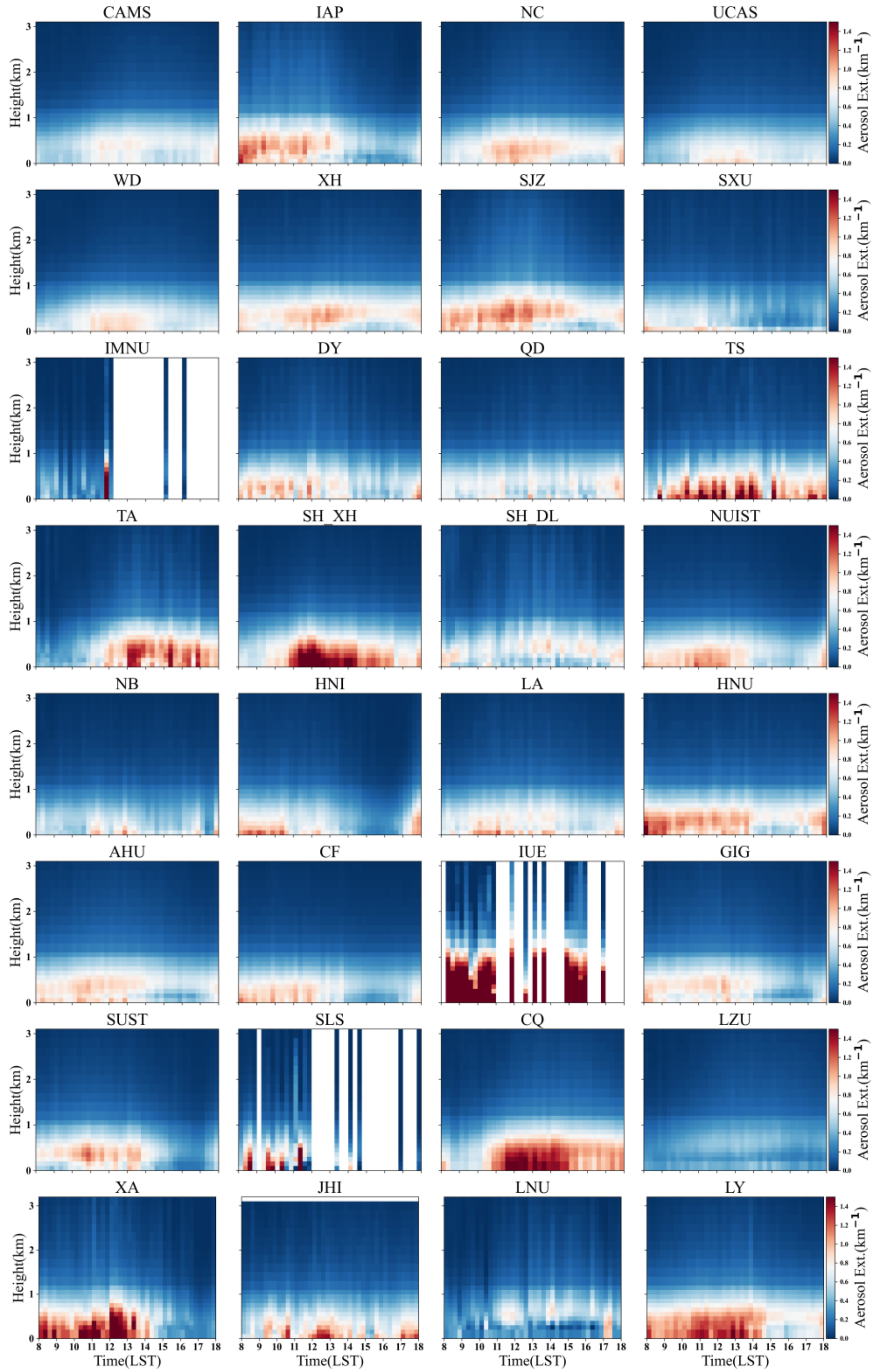

Figure S9. Diurnal variation of the summer averaged aerosol extinction vertical profiles during 2019-2023.

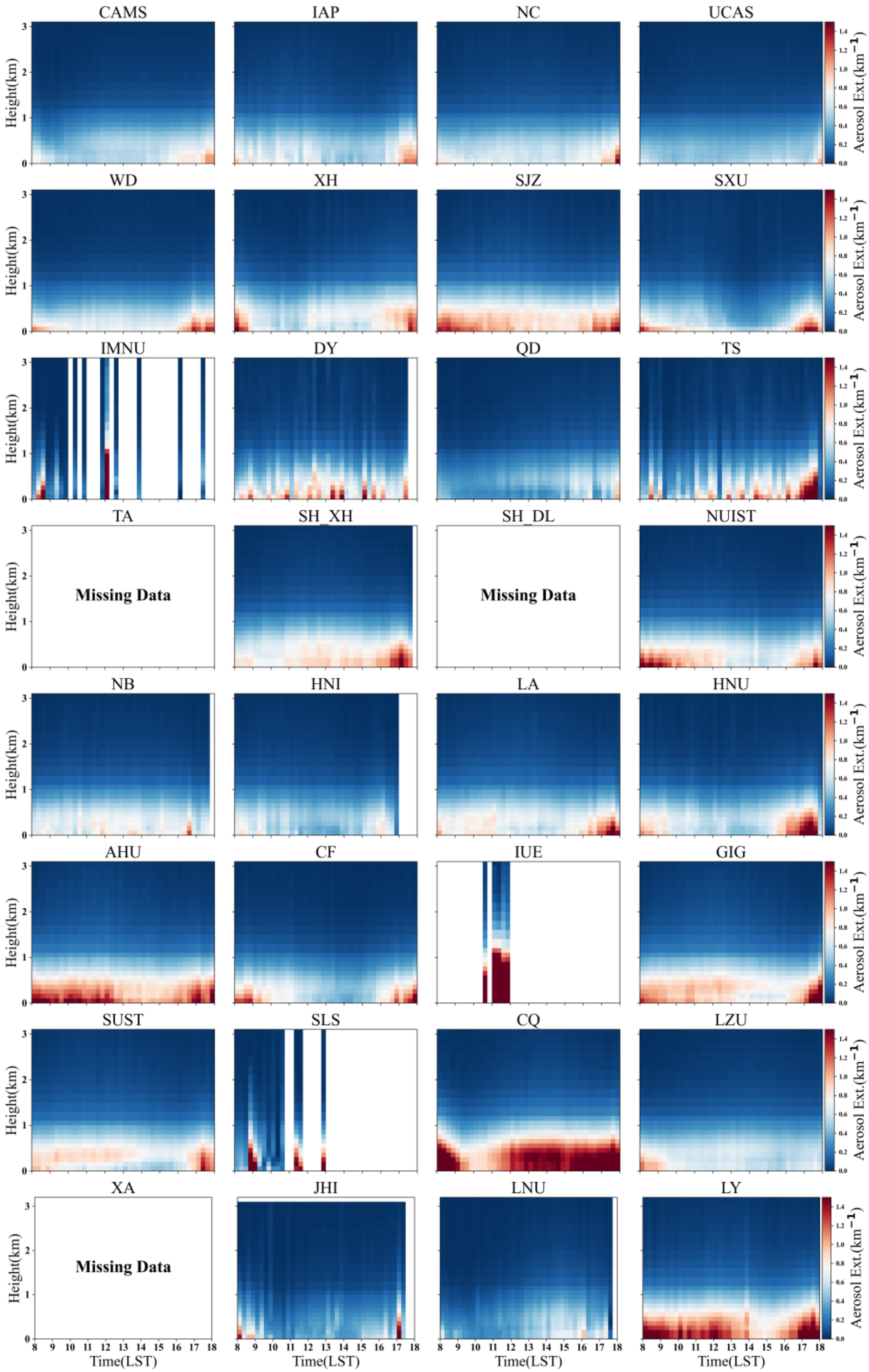

Figure S10. Diurnal variation of the autumn averaged aerosol extinction vertical profiles during 2019-2023.

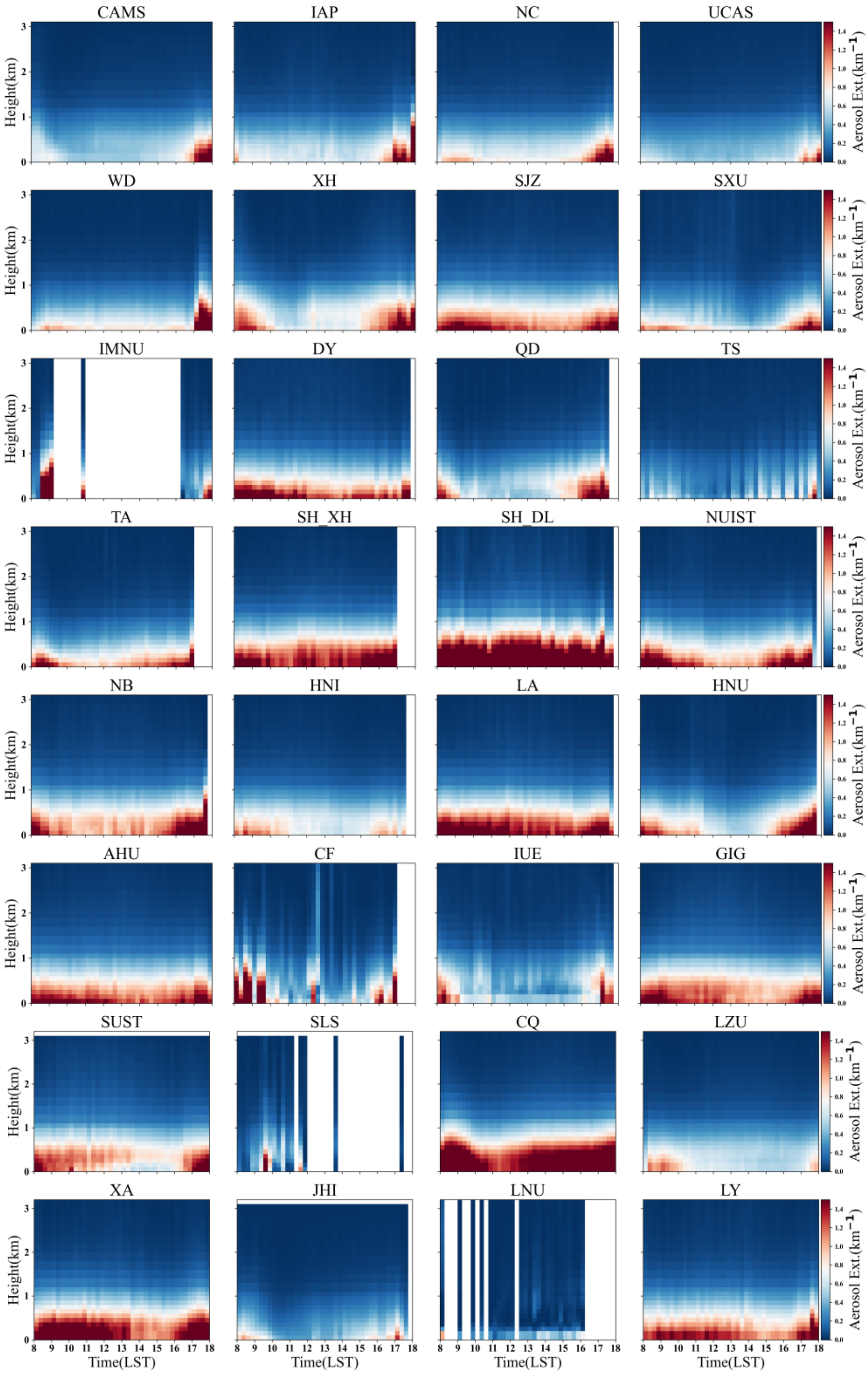

75 **Figure S11. Diurnal variation of the winter averaged aerosol extinction vertical profiles during 2019-2023.**

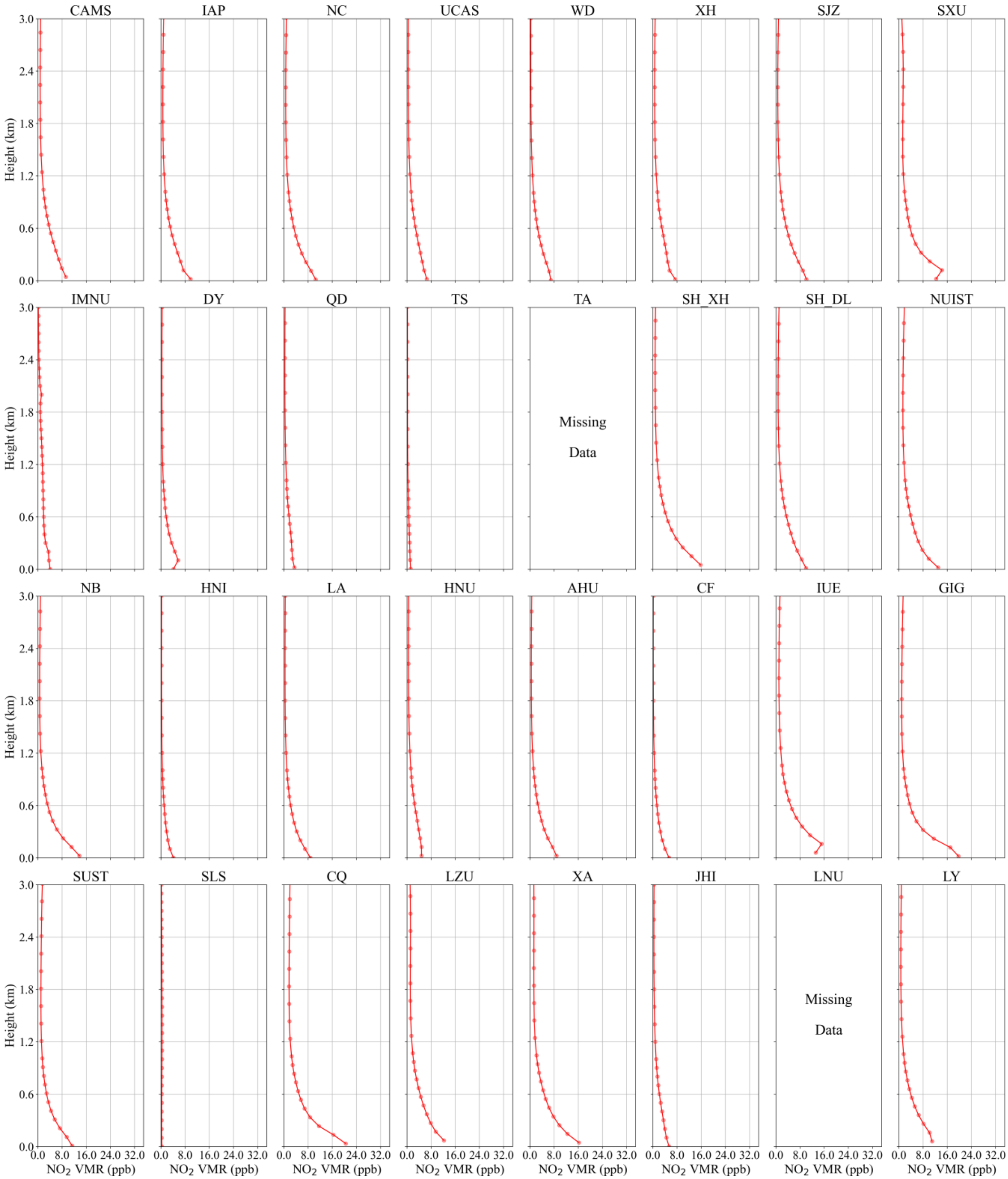

Figure S12. Spring averaged NO_2 vertical profiles during 2019-2023.

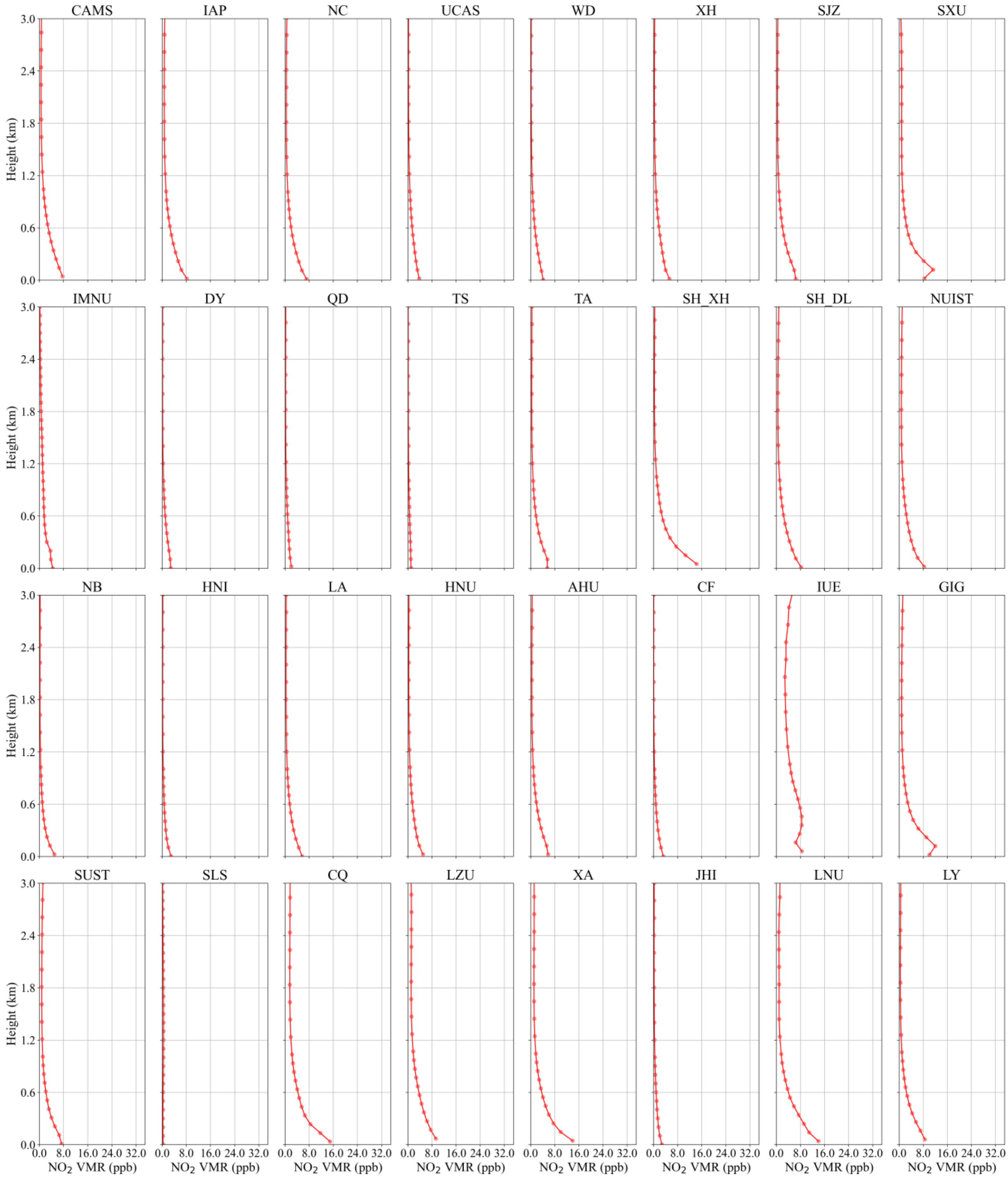

Figure S13. Summer averaged NO_2 vertical profiles during 2019-2023.

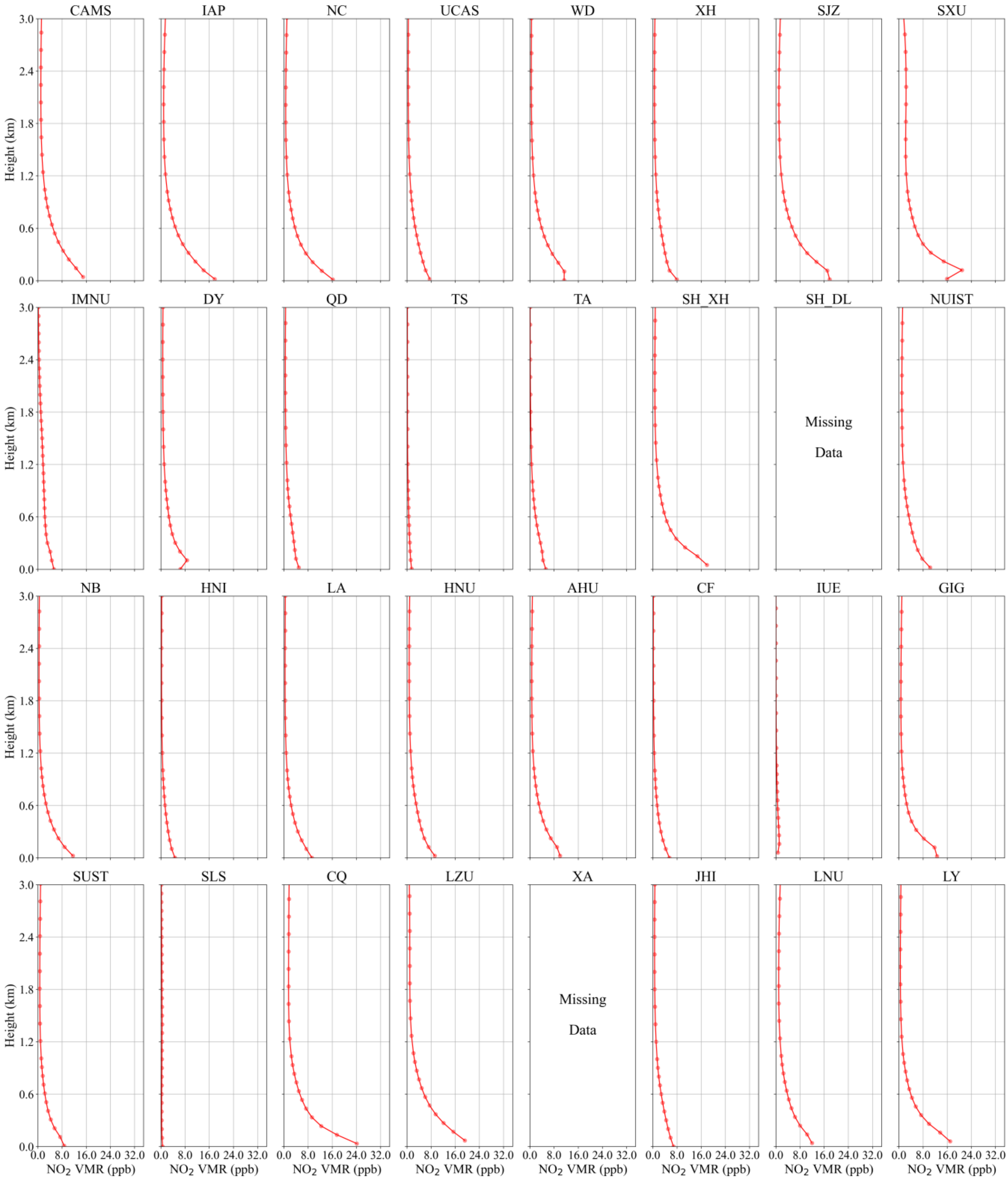

80 **Figure S14. Autumn averaged NO_2 vertical profiles during 2019-2023.**

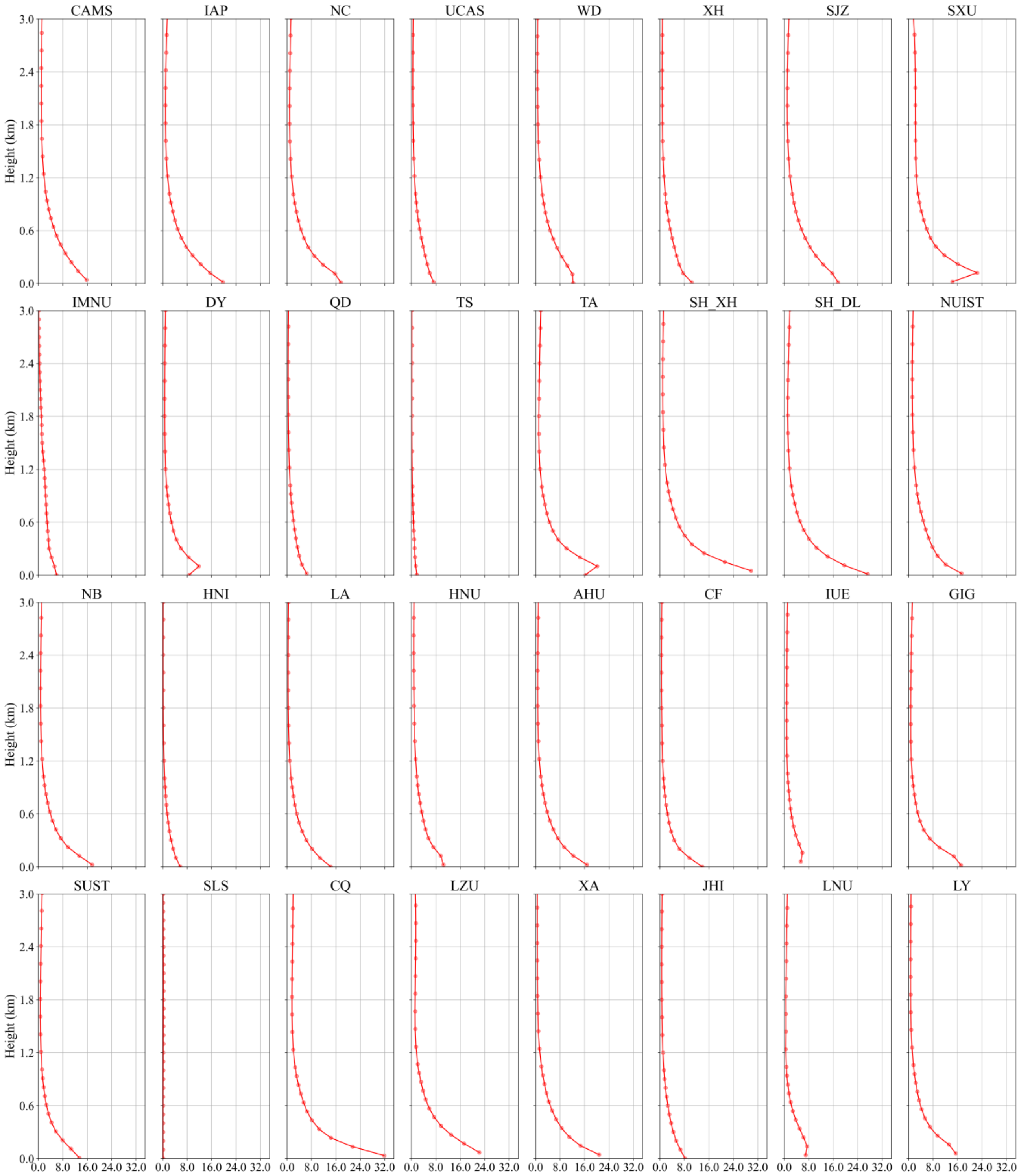

Figure S15. Winter averaged NO_2 vertical profiles during 2019-2023.

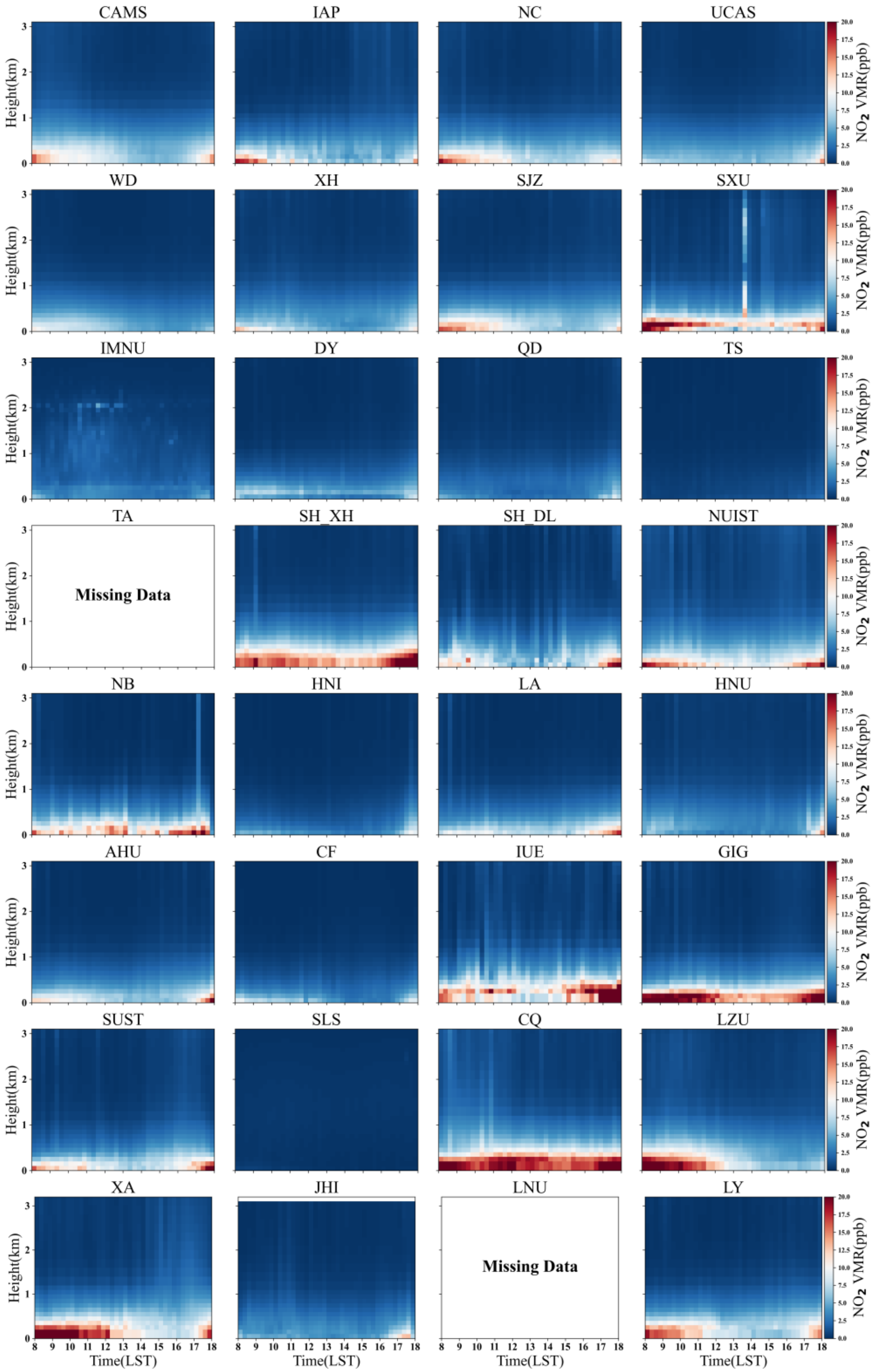

Figure S16. Diurnal variation of the spring averaged NO_2 vertical profiles during 2019-2023.

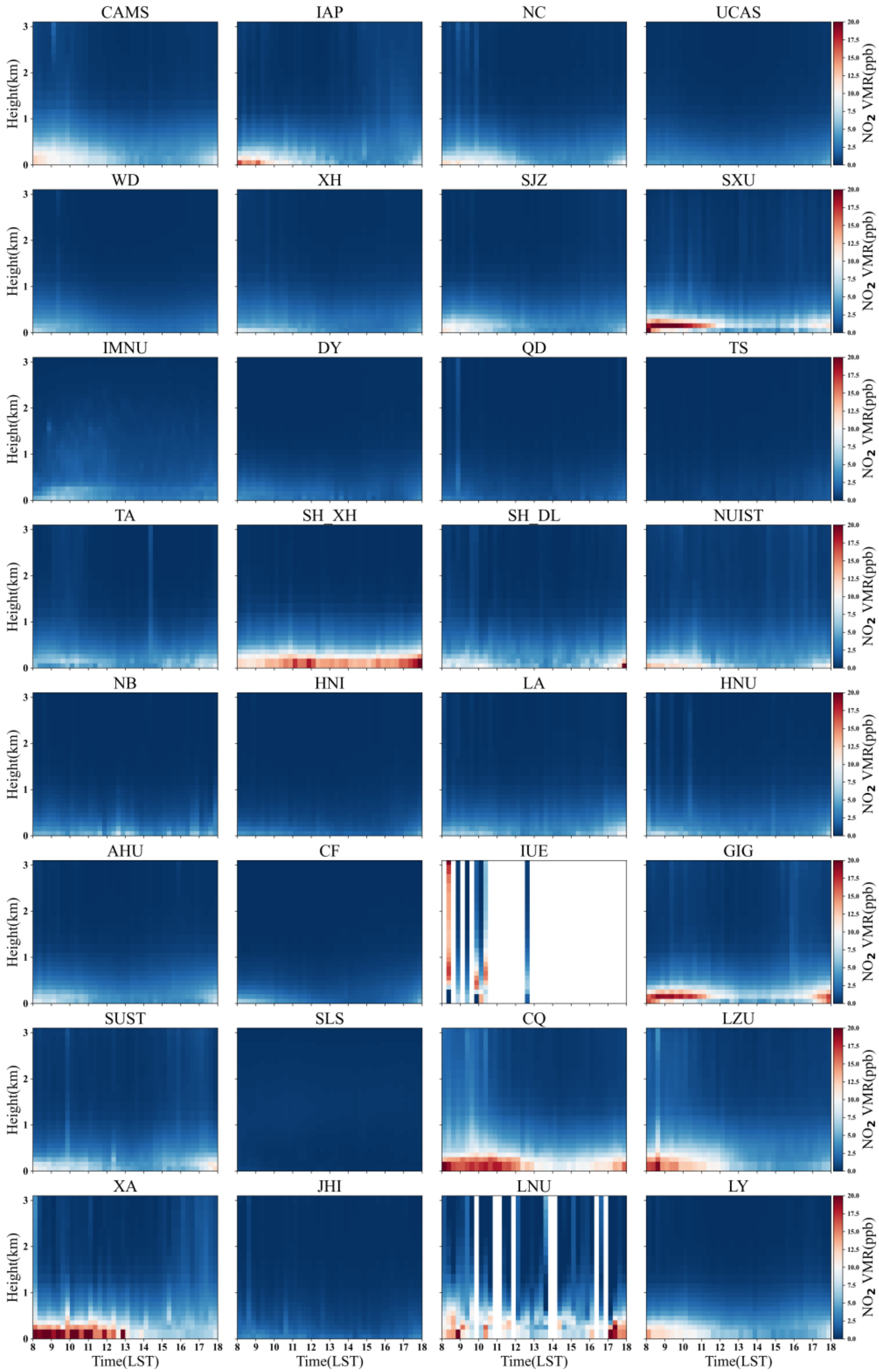

Figure S17. Diurnal variation of the summer averaged NO_2 vertical profiles during 2019-2023.

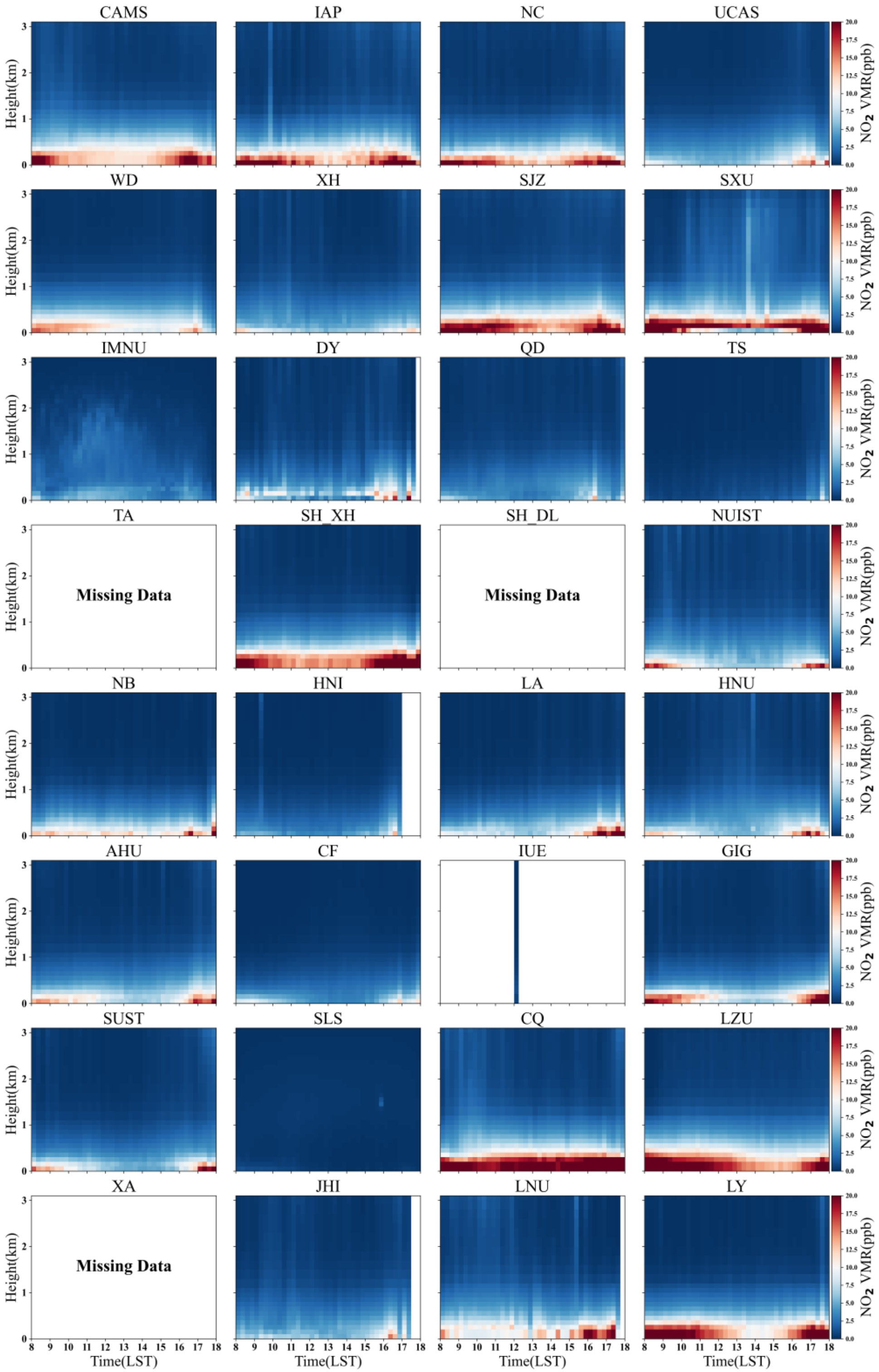

Figure S18. Diurnal variation of the autumn averaged NO_2 vertical profiles during 2019-2023.

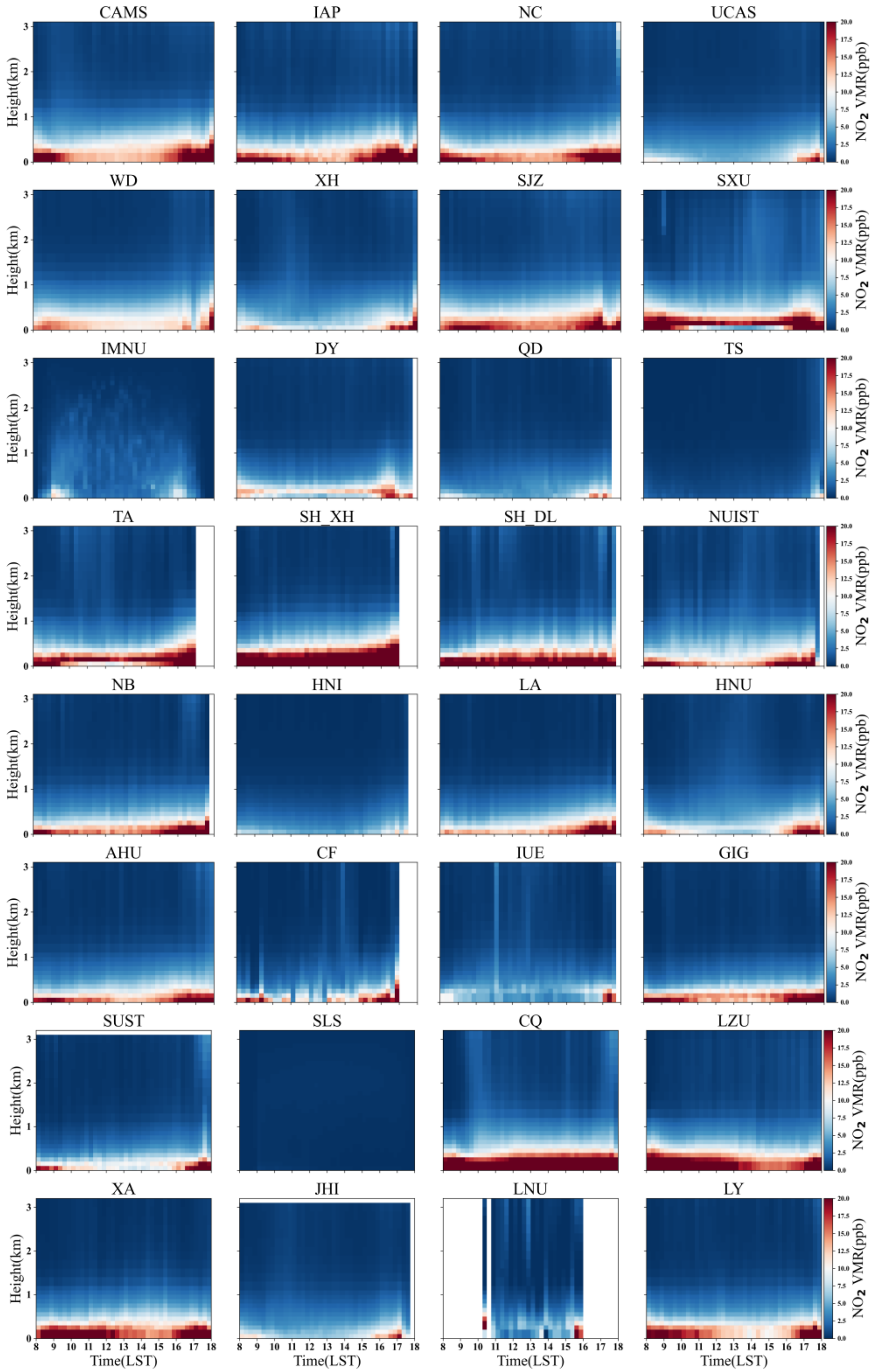

Figure S19. Diurnal variation of the winter averaged NO_2 vertical profiles during 2019-2023.

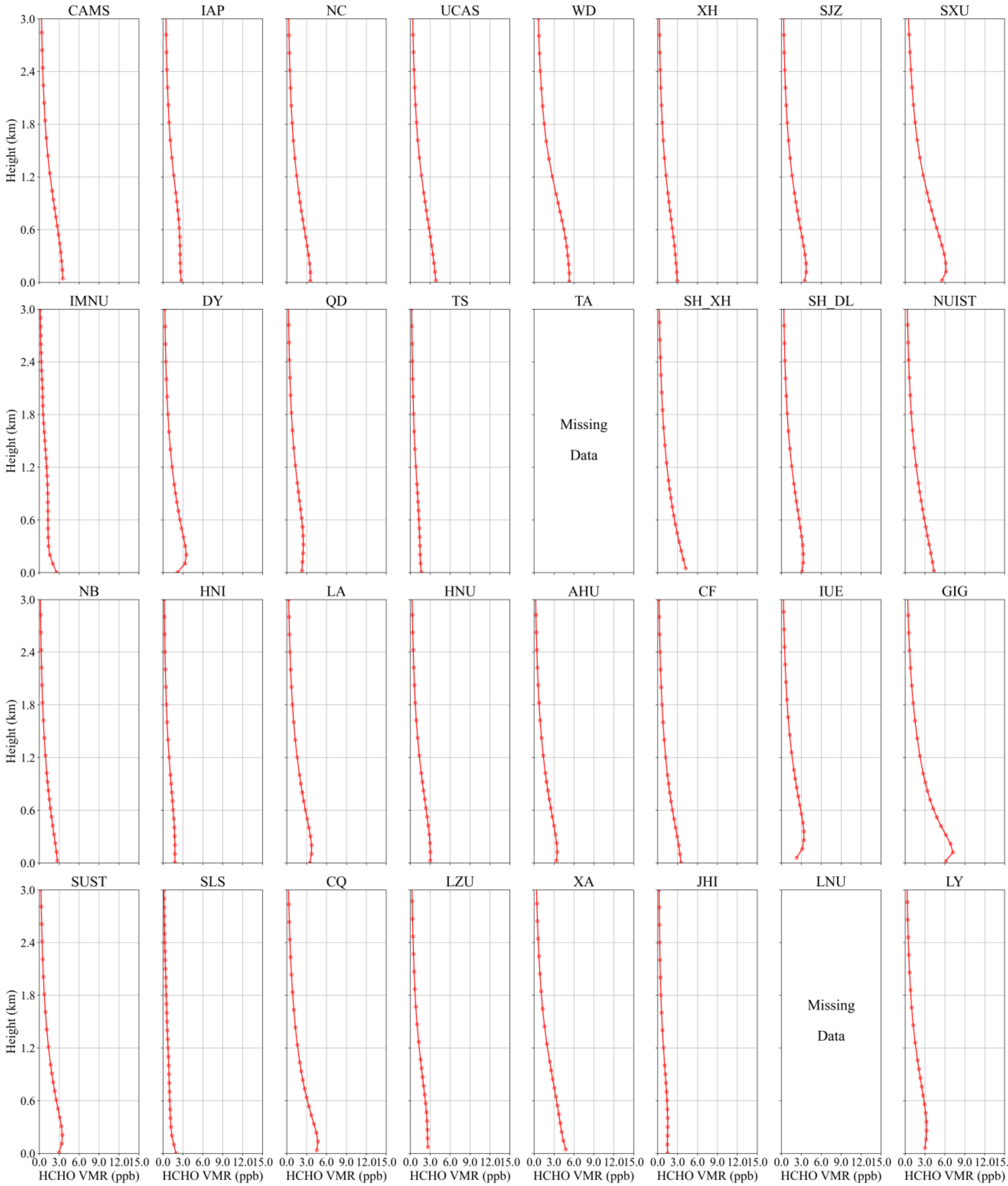

Figure S20. Spring averaged HCHO vertical profiles during 2019-2023.

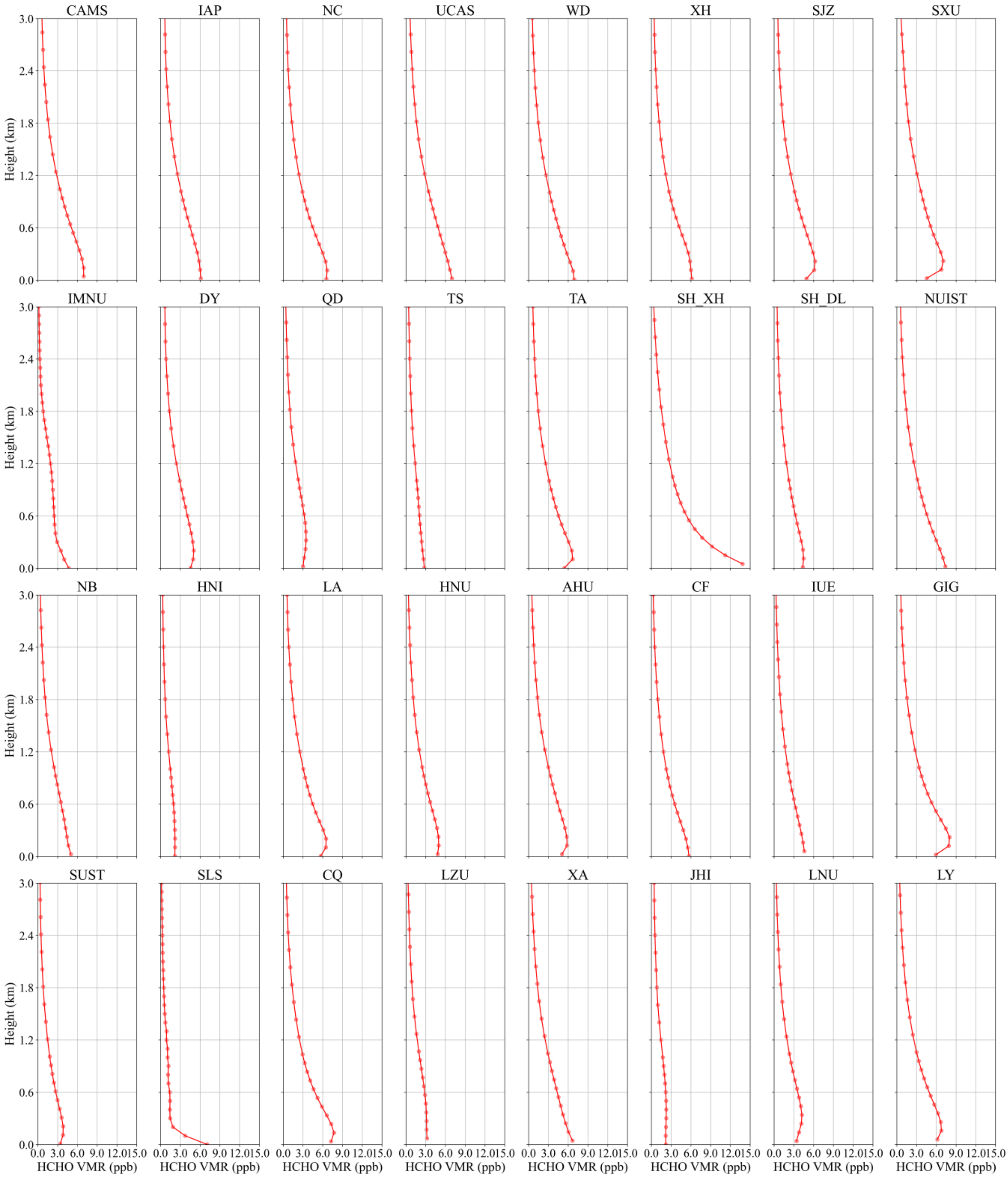

95 **Figure S21. Summer averaged HCHO vertical profiles during 2019-2023.**

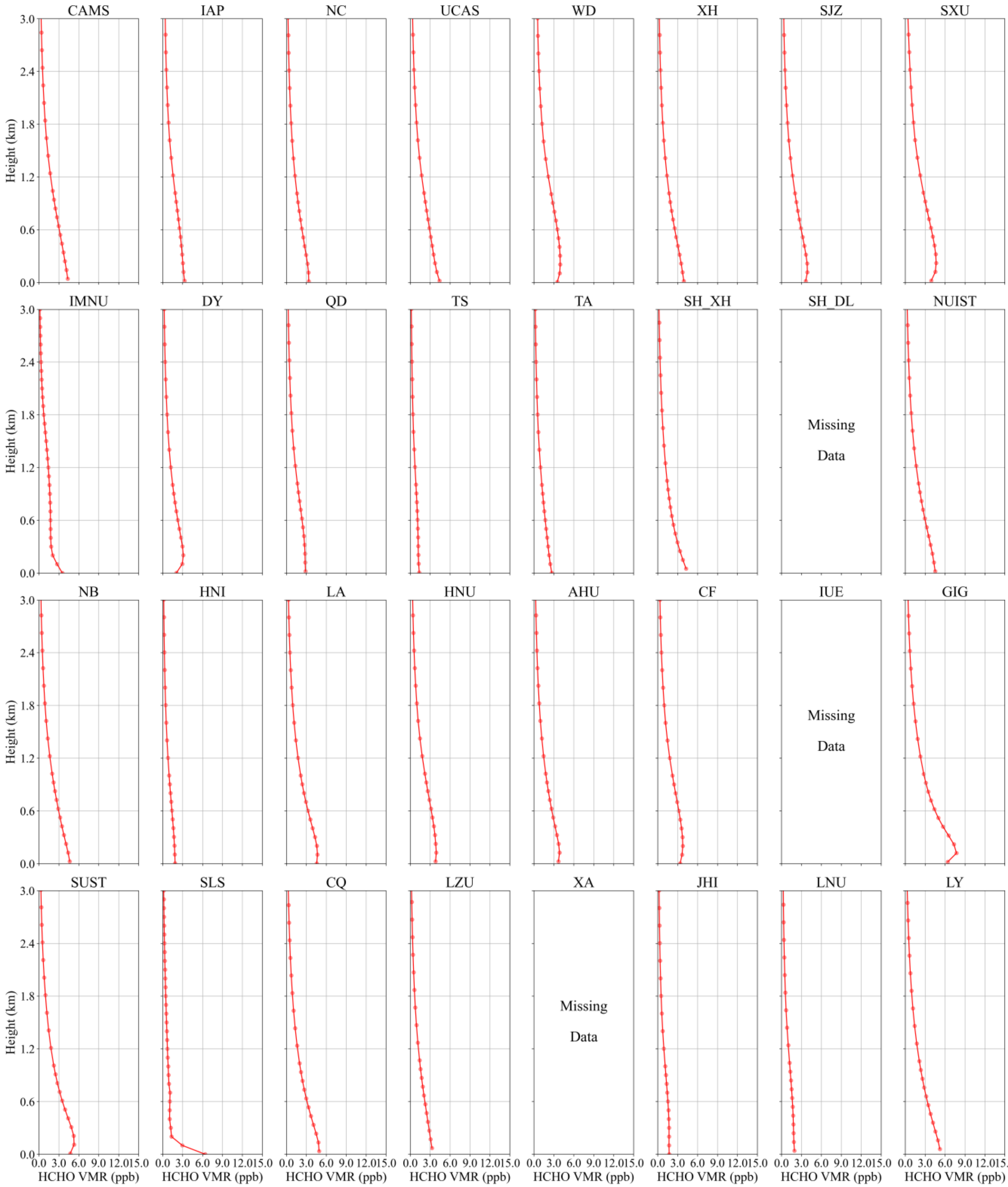

Figure S22. Autumn averaged HCHO vertical profiles during 2019-2023.

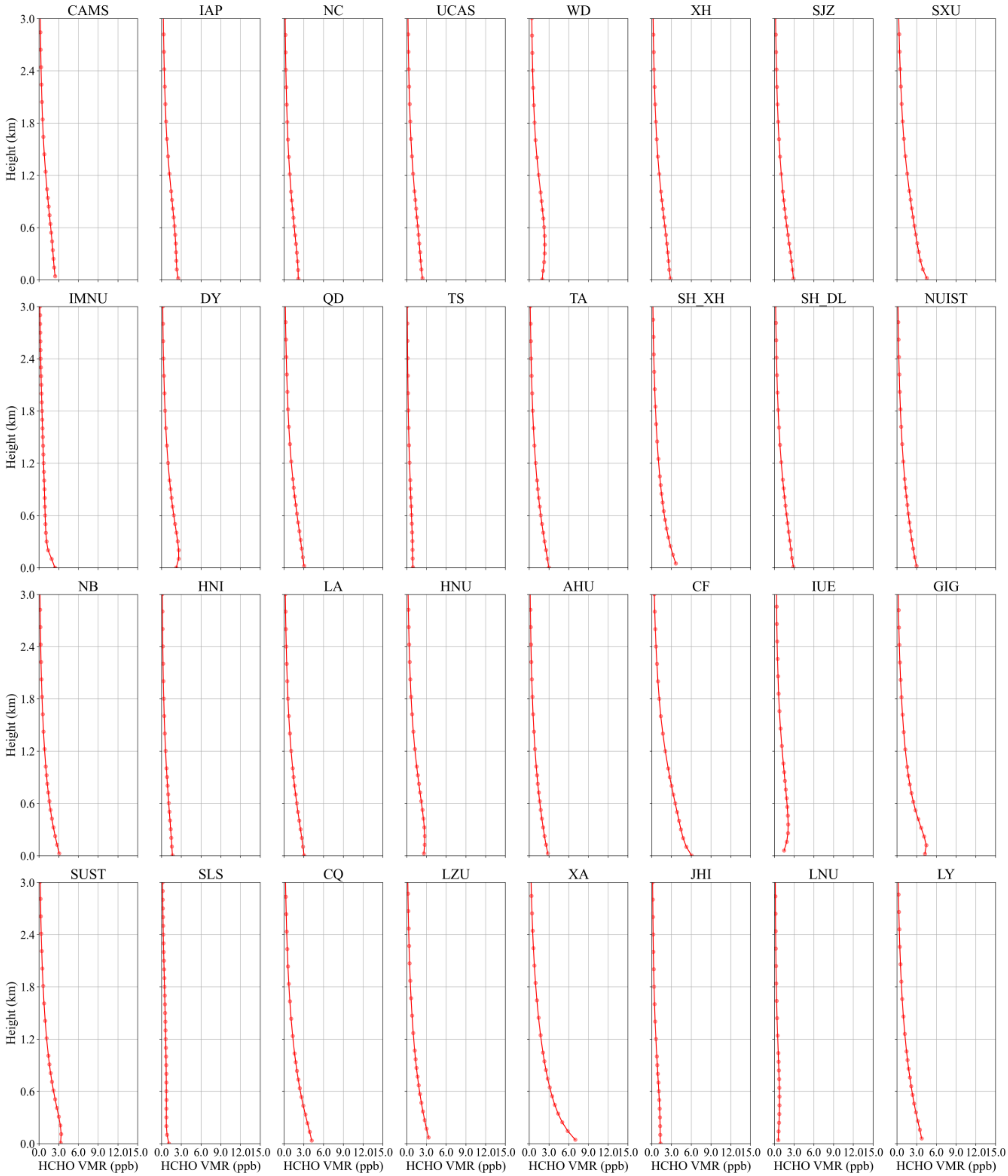

Figure S23. Winter averaged HCHO vertical profiles during 2019-2023.

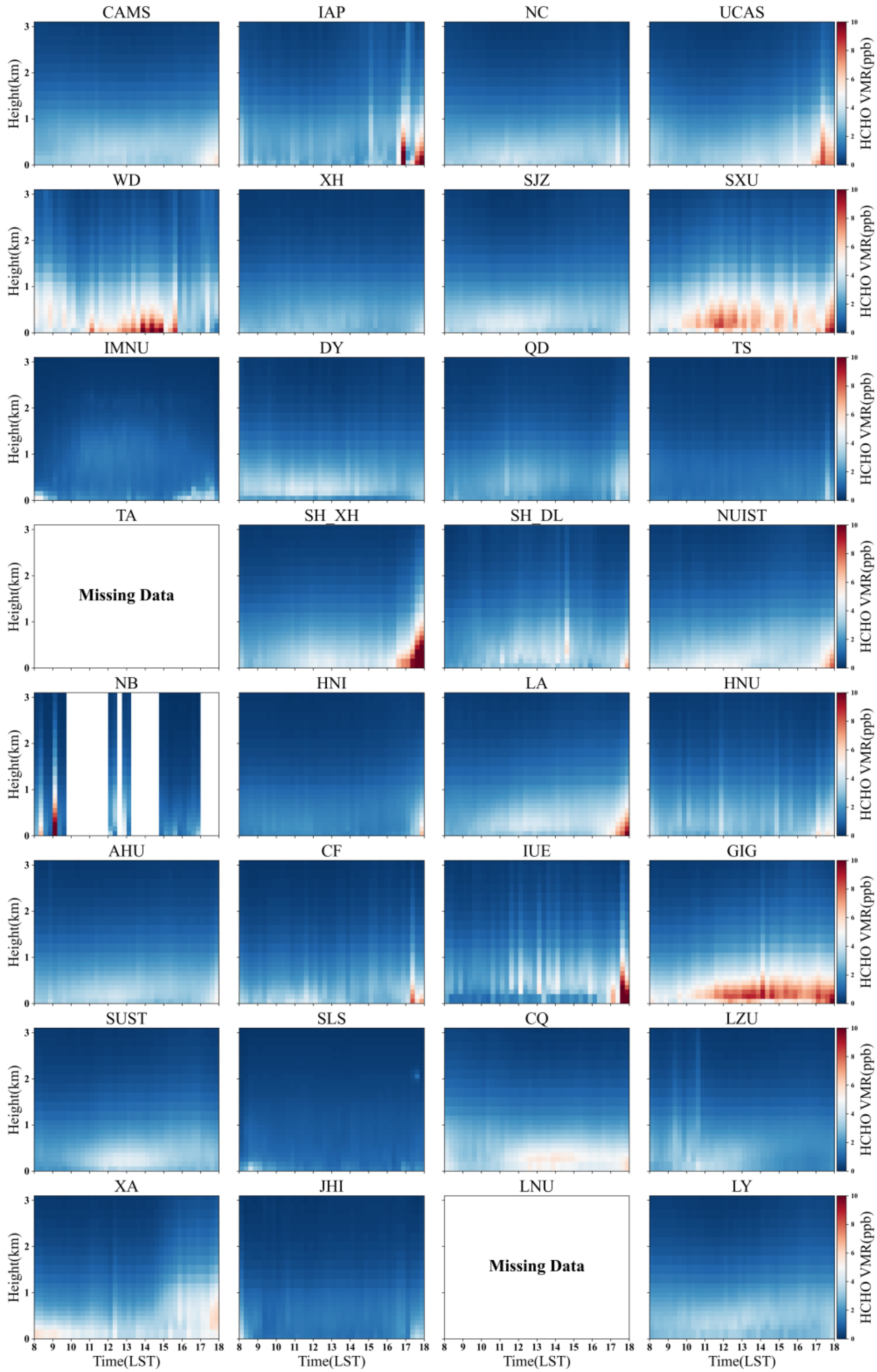

Figure S24. Diurnal variation of the spring averaged HCHO vertical profiles during 2019-2023.

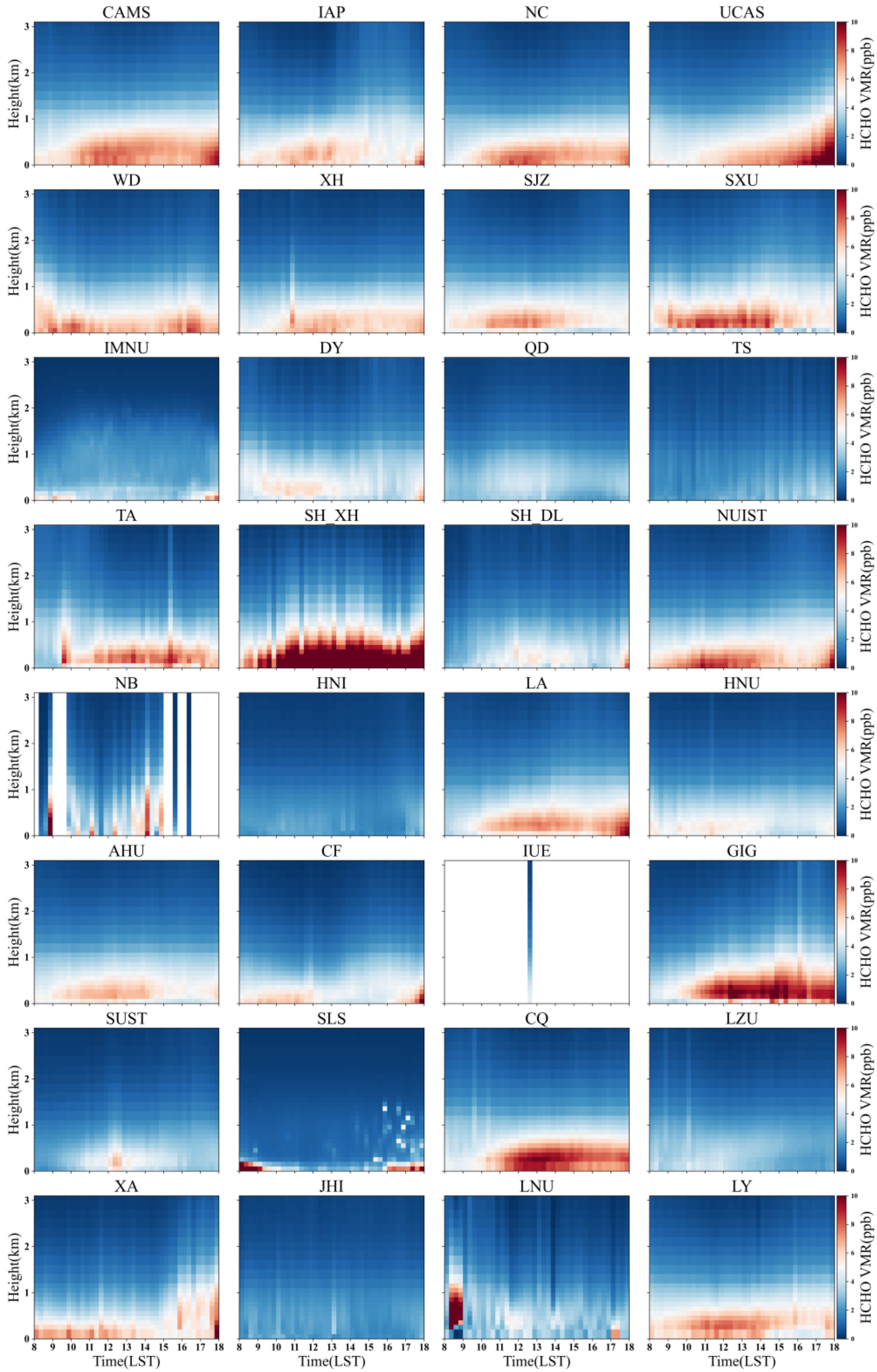

Figure S25. Diurnal variation of the summer averaged HCHO vertical profiles during 2019-2023.

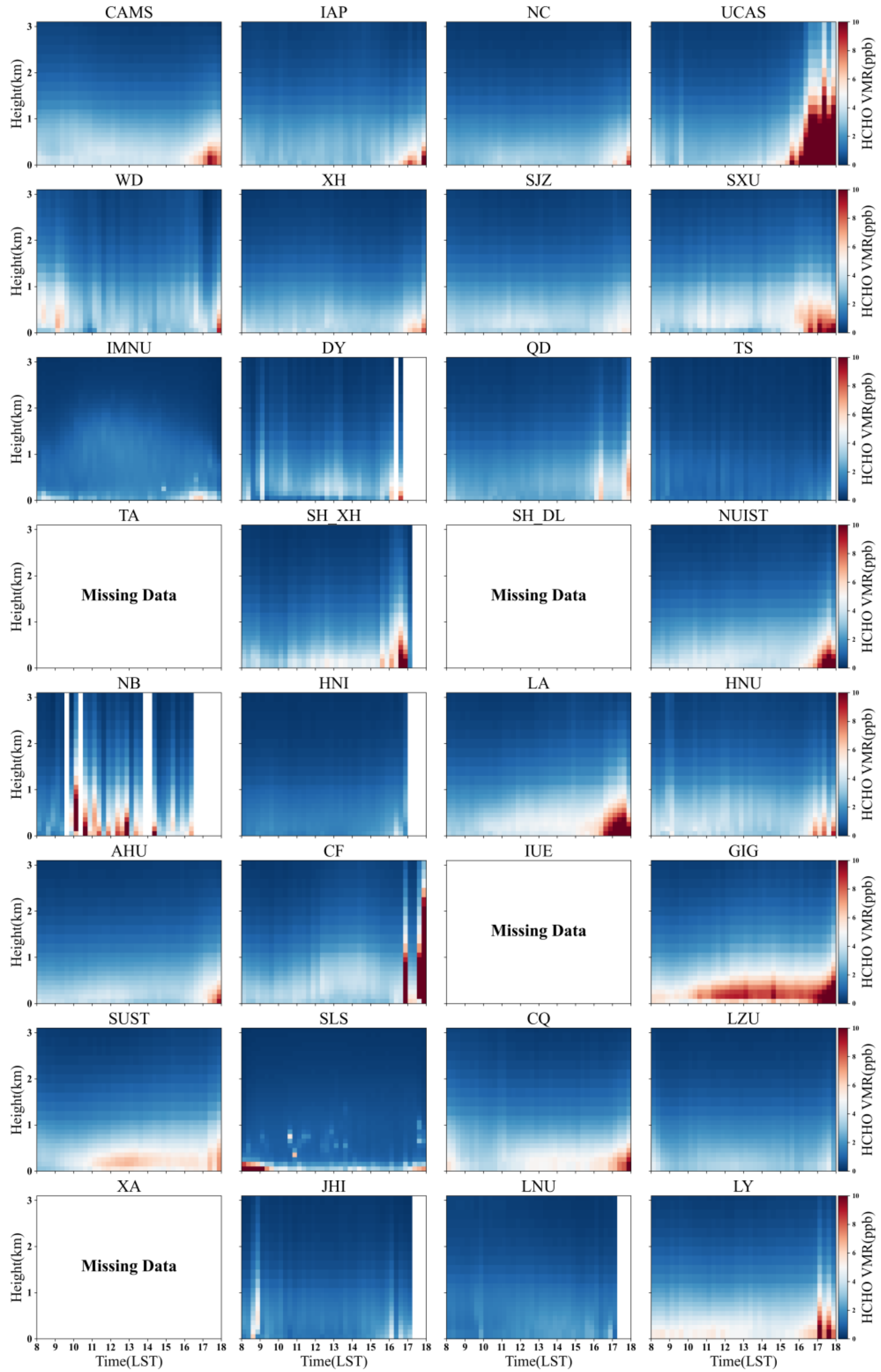

Figure S26. Diurnal variation of the autumn averaged HCHO vertical profiles during 2019-2023.

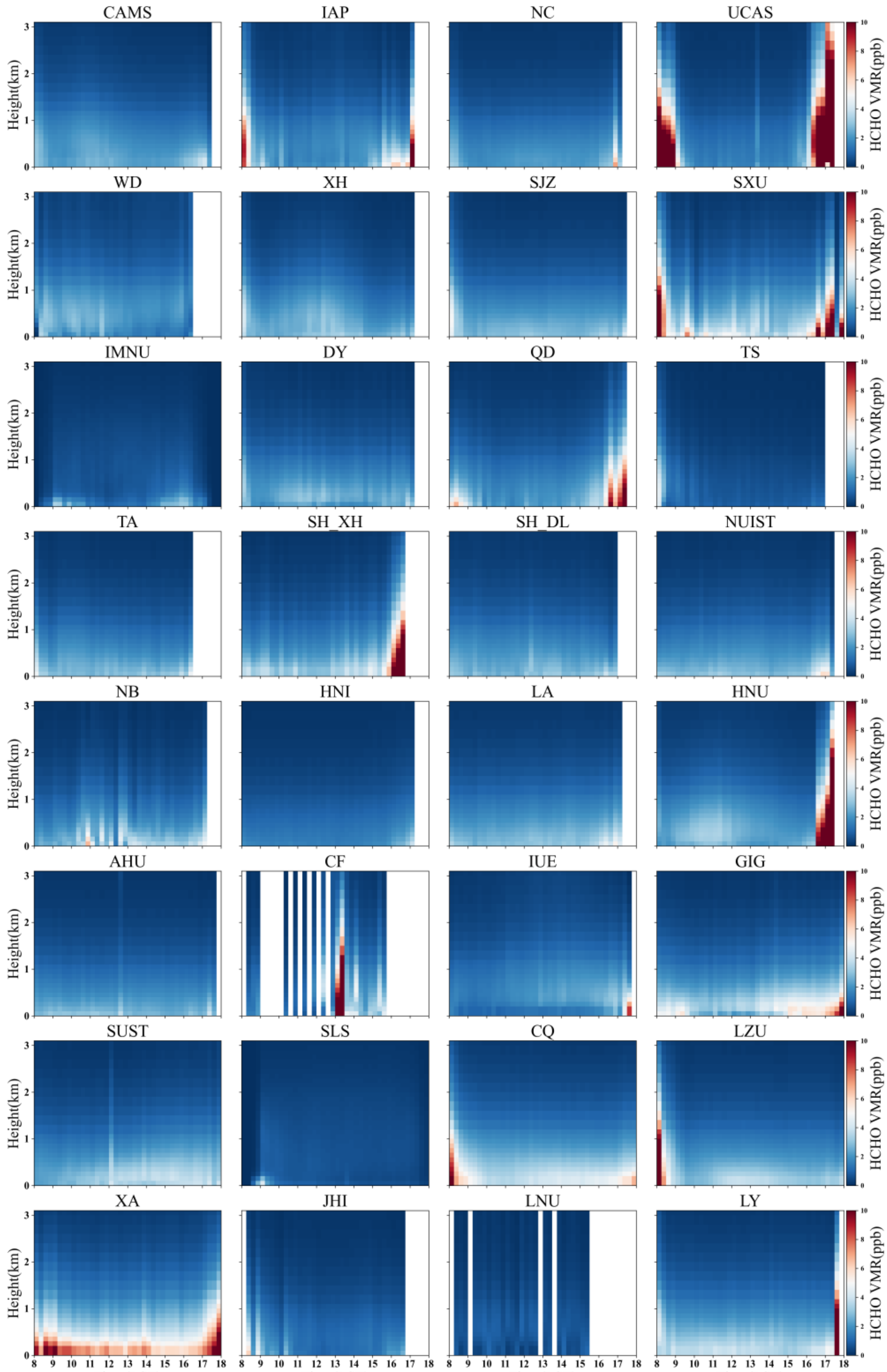

Figure S27. Diurnal variation of the winter averaged HCHO vertical profiles during 2019-2023.

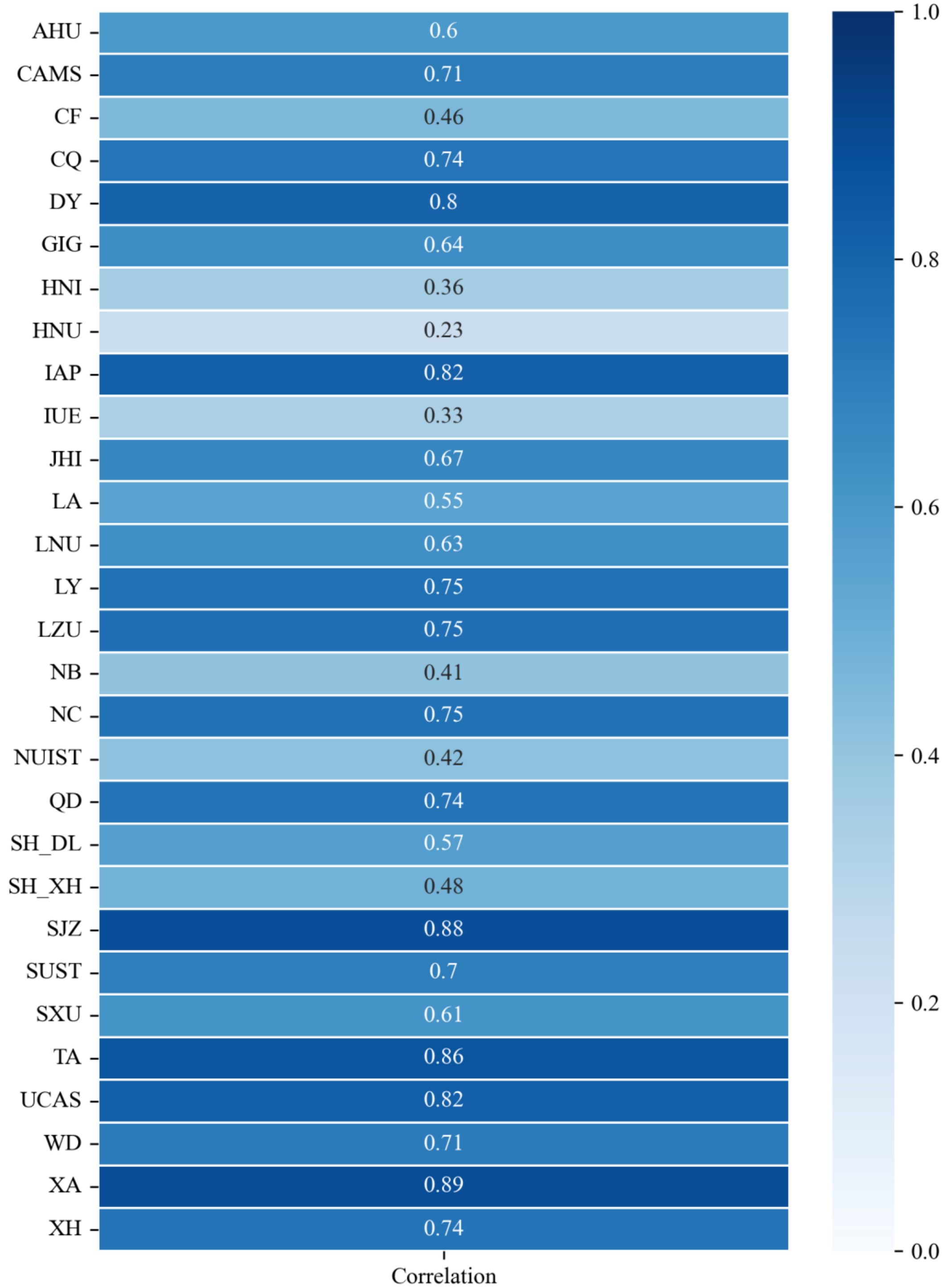

Figure S28. Correlation of surface AEC measured at each site and PM2.5 measured by CNEMC.

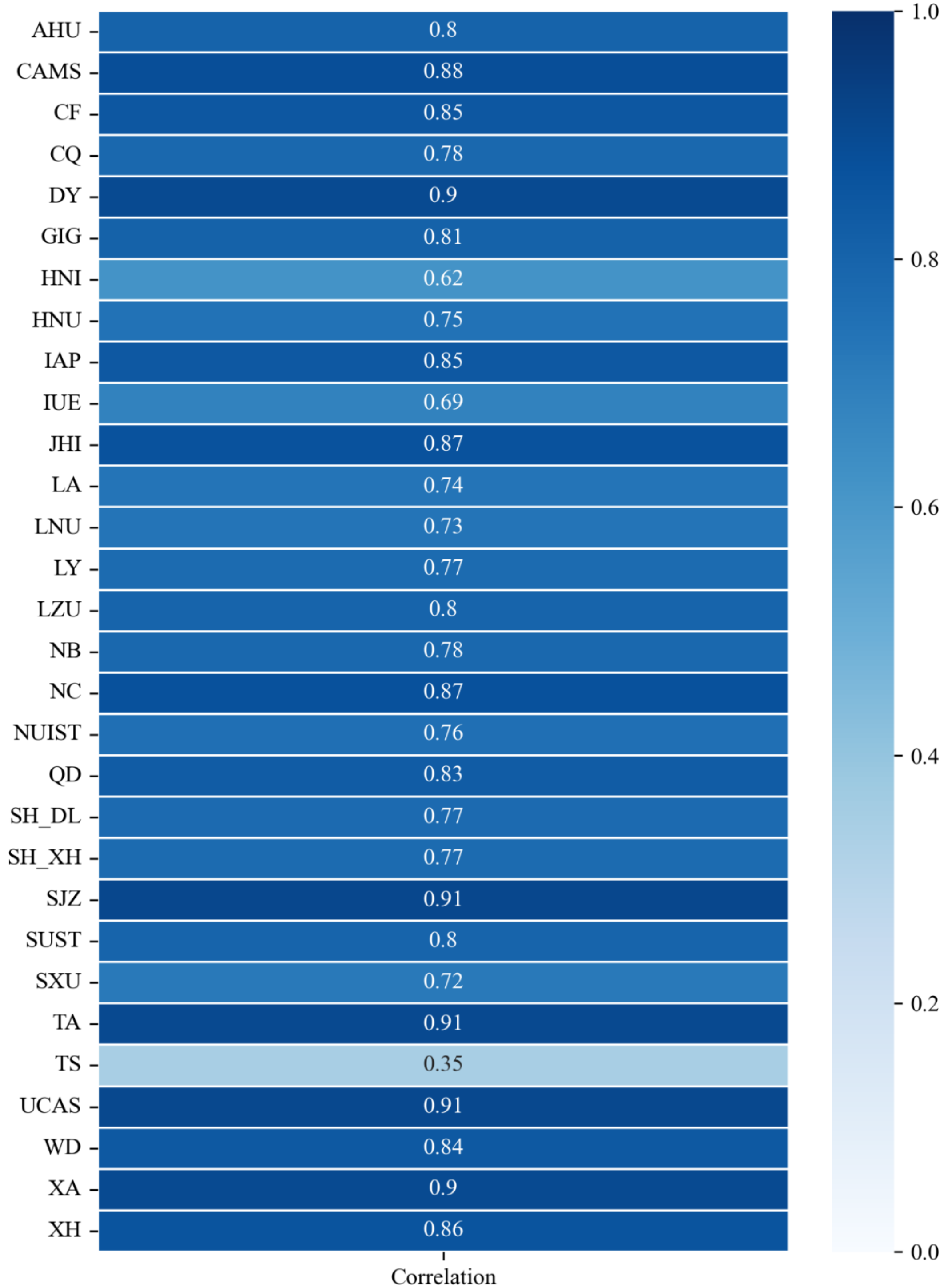

Figure S29. Correlation of NO_2 concentration measured by each site and CNEMC.

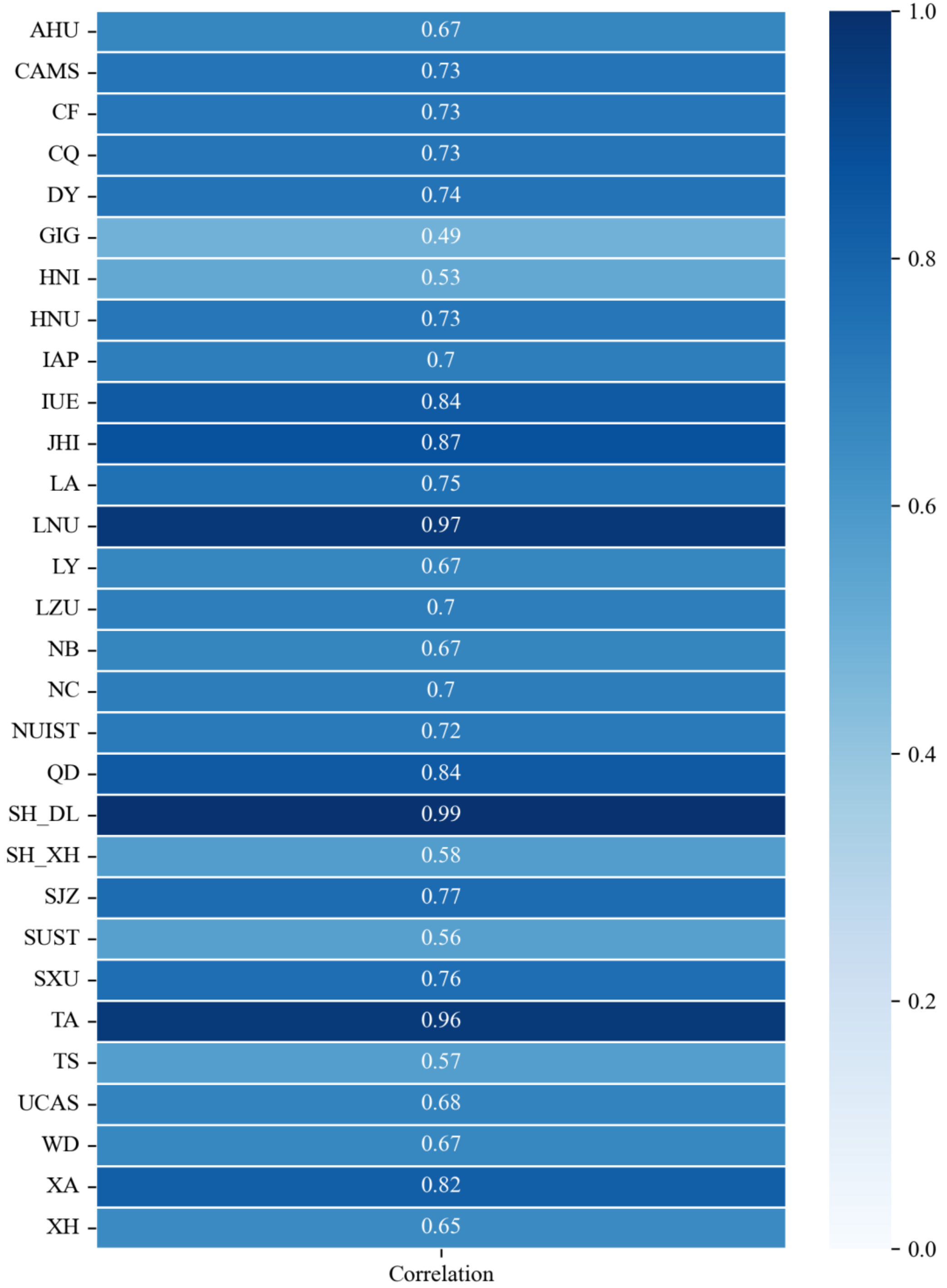

Figure S30. Correlation of tropospheric NO_2 VCD measured by each site and TROPOMI.

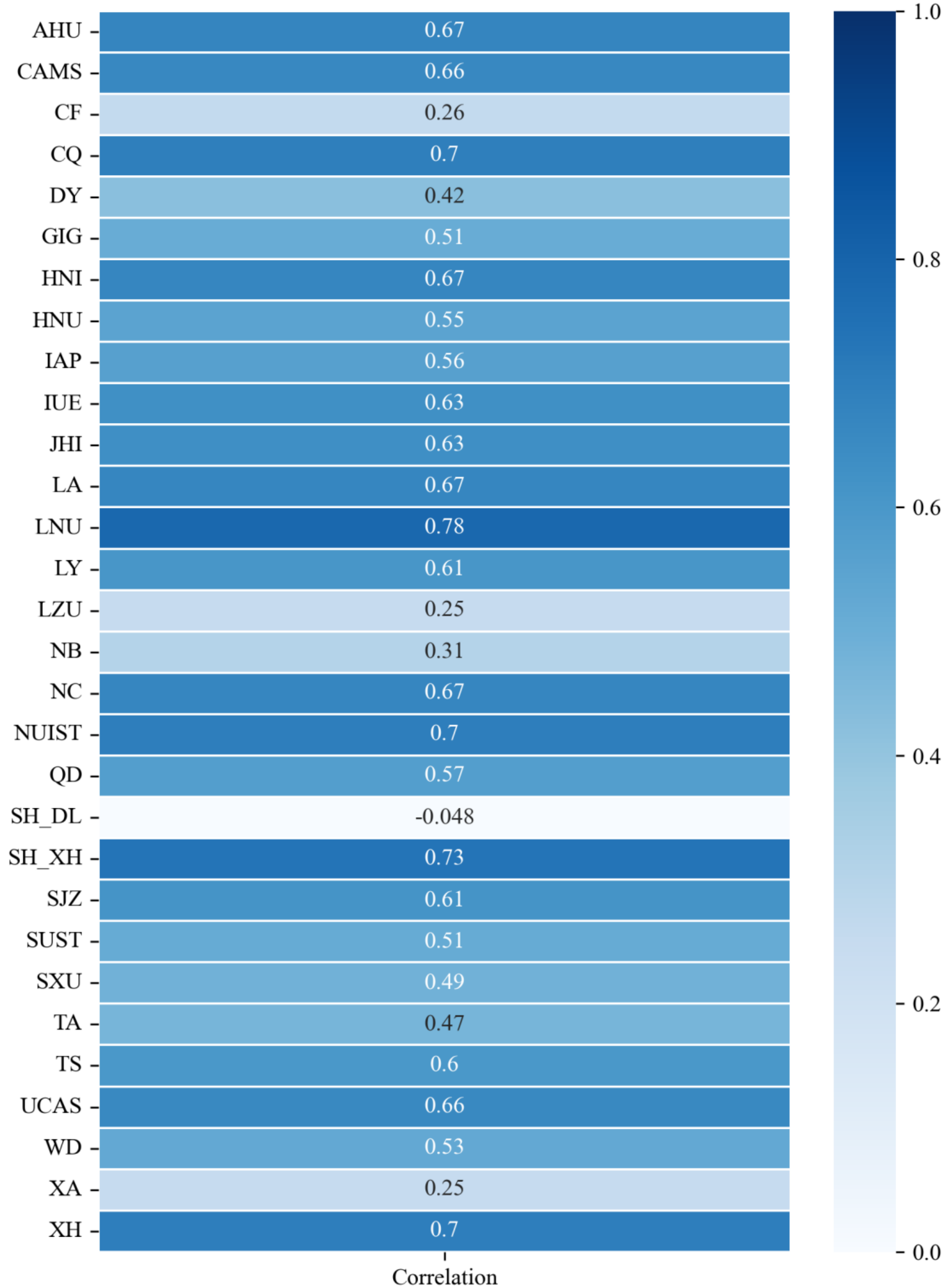

Figure S31. Correlation of tropospheric HCHO VCD measured by each site and TROPOMI